

UNIVERSITY OF CRETE

SCHOOL OF SCIENCES AND ENGINEERING

DEPARTMENT OF CHEMISTRY



Department of Materials Science and Technology

Laboratory of Synthetic Biomaterials

Bachelor Thesis

**“Synthesis of fluorinated protein-polymer conjugates via an
oxygen tolerant copper catalyzed RDRP method”**

Eva Hatzivasiliou

Supervisor: Assistant Professor Kelly Velonia

HERAKLION 2019

Acknowledgements

I owe a big thank you to my supervisor, assistant professor Kelly Velonia, who gave me the opportunity to conduct my bachelor thesis in the Laboratory of Synthetic Biomaterials and be an active member of her research group. Her guidance throughout this year was really helpful and crucial for the accomplishment of all the work described in this thesis.

I would also like to thank the postdoctoral researcher Alexis Theodorou. His important advice and guidance gave me the necessary knowledge and skills for my further academic progress. The valuable time that he spend for my undergraduate thesis were crucial for the successful fulfilment of this work.

Moreover, I would like to thank the postdoctoral researcher Charis Gryparis, who was always present along with the master student Peter Mandriotis, when I needed their support and useful assistance.

Finally, I would like to thank all the members of my laboratory for the pleasant work environment. More specifically I thank Dimitri Gounari, Chrysi Baltzaki, Mary Papageorgiou, Elina Koi, Sofia Koutandou, Marilena Youlouda and Iro Papagiannaki

The biggest thank you is something I owe to my family who always support me with everything I do in my life!

Abbreviations

ATRA	Atom Transfer Radical Addition
ATRP	Atom Transfer Radical Polymerization
BSA	Bovine Serum Albumin
CRP	Controlled Radical Polymerization
CuAAC	Copper alkyne-azide cycloaddition
CYL	Cylindrical micelles
DMSO	Dimethyl Sulfoxide
EBiB	Ethyl α -bromoisobutyrate
EDTA	Ethylenediaminetetraacetic acid
GPC	Gel Permeation Chromatography
HEX	Hexagonally ordered cylinders
HFIPMA	1,1,1,3,3,3-hexafluoroisopropyl methacrylate
HPL	Hexagonally Perforated Layers
IR	Infrared
LAM	Lamellae
LRP	Living Radical Polymerization
Me ₆ TREN	Tris[2-(dimethylamino)ethyl]amine
MIC	Spherical micelles
MLAM	Modulated Lamellae
MRI	Magnetic Resolution Imaging
MWCO	Molecular Weight Cut-Off
NMP	Nitroxide-Mediated Polymerization
NMR	Nuclear Magnetic Resonance
PAGE	Polyacrylamide Gel Electrophoresis
PFCE	Perfluoron-Crown Ether
PFCs	Perfluorocarbons
PFPE	Perfluoropolyether
PMMA	Poly-Methyl Metacrylate
PS- <i>b</i> -PAA	Polystyrene- <i>b</i> -poly(acrylic acid)
RAFT	Reversible Addition/Fragmentation

SET-LRP	Chain Transfer Polymerization Single Electron Transfer - Living Radical Polymerization
TBAF	Tetra-n-butylammonium fluoride
TFEA	2,2,2-trifluoroethyl acrylate
TFEMA	2,2,2-trifluoroethyl methacrylate
THF	Tetrahydrofuran
TLC	Thin Layer Chromatography
UV Vis	Ultra Violet Visible

ABSTRACT

Fluorinated polymers have already been applied in a variety of real life issues due to their unique chemical characteristics. However, their inherent properties also have some drawbacks and especially their solvophobicity causes significant problems on their use. Therefore, our laboratory is involved with the synthesis of a new class protein-fluorinated polymer bioconjugates targeting to more biological applications such as magnetic resolution imaging and drug delivery systems.

The purpose of this thesis was to synthesize amphiphilic fluorinated polymer bioconjugates following new oxygen tolerant methods. A variety of fluorinated monomers were utilized for the development of different polymer chains onto the protein, following polymerization techniques catalyzed by copper that do not require the deoxygenation of the system (RDRP). In detail, two experimental approaches were followed, the single electron transfer - living radical polymerization (SET-LRP) and photo-induced living radical polymerization using UV lamp. The classical procedures were slightly altered through the use of syringe in order to limit the presence of oxygen and do not apply any deoxygenation procedure, simply by eliminating the reaction headspace. Our goal was to optimize the synthetic protocols, expand their use with new monomers and utilize ^{19}F -NMR and IR spectroscopy for their characterization, in order to fully comprehend the properties of this new category of protein polymer conjugates .

ΠΕΡΙΛΗΨΗ

Τα φθοριωμένα πολυμερή έχουν ήδη βρει ποικίλες εφαρμογές σε προβλήματα της καθημερινής ζωής λόγω των μοναδικών χημικών τους ιδιοτήτων. Παρόλα αυτά οι εγγενείς τους ιδιότητες έχουν και ορισμένα μειονεκτήματα και ιδιαίτερα η μικρή διαλυτότητα που έχουν στους περισσότερους οργανικούς διαλύτες και στο νερό δυσχεραίνει την χρήση τους. Για αυτό το λόγο στο εργαστήριό μας αναπτύσσονται μέθοδοι σύνθεσης μιας νέας τάξης φθοριωμένων πολυμερών, συζευγμένων με πρωτεΐνες με ποικίλες πιθανές βιολογικές εφαρμογές όπως η μαγνητική τομογραφία και η ελεγχόμενη μεταφορά φαρμάκων.

Σκοπός της παρούσας πτυχιακής εργασίας είναι η σύνθεση αμφίφιλων φθοριωμένων βιοπολυμερών ακολουθώντας νέες συνθετικές μεθόδους όπου γίνεται απομάκρυνση του υπερκείμενου χώρου στο δοχείο της αντίδρασης. Μια ποικιλία από φθοριωμένα μονομερή χρησιμοποιήθηκαν για την ανάπτυξη διαφορετικών πολυμερικών αλυσίδων πάνω στην πρωτεΐνη, ακολουθώντας τεχνικές ριζικού πολυμερισμού με αντιστρεπτή απενεργοποίηση (RDRP) καταλυόμενες από χαλκό, που δεν απαιτούν αποξυγόνωση του συστήματος. Πιο συγκεκριμένα, ακολουθήθηκαν δύο πειραματικές προσεγγίσεις, εκείνη της ανακατανομής καθώς και ο φωτοεπαγόμενος ριζικός πολυμερισμός με λάμπα υπεριώδους. Ως δοχεία των αντιδράσεων χρησιμοποιήθηκαν πλαστικές σύριγγες πολυπροπενίου που επιτρέπουν την απομάκρυνση του υπερκείμενου χώρου, πιέζοντας απλά το έμβολο της σύριγγας. Βασικός στόχος μας ήταν η βελτιστοποίηση των πειραματικών πρωτοκόλλων, η χρήση της μεθόδου σε νέα μονομερή και η αξιοποίηση του ^{19}F -NMR και IR για τον χαρακτηρισμό των συζυγών πρωτεΐνης-πολυμερούς.

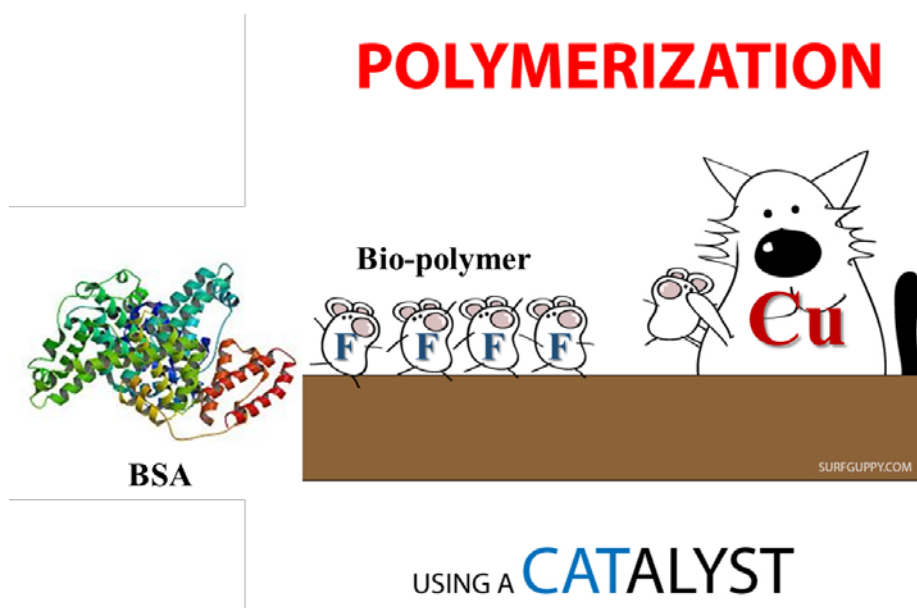


TABLE OF CONTENTS

Chapter 1: Introduction	9
1.1 Fluorinated polymers	9
1.2 Amphiphilic molecules	10
1.3 Giant Amphiphiles	11
1.4 Self-assembly	13
1.5 ATRP (Atom Transfer Radical Polymerization)	14
1.6 SET-LRP (Single Electron Transfer - Living Radical Polymerization)	16
1.7 Photo-induced Living Radical Polymerization	17
Chapter 2: Aims of the Thesis	19
Chapter 3: Synthetic approaches	21
Chapter 4: Results and Discussion	22
4.1 Synthesis of 4-(2-Hydroxyethyl)-10-oxa-4-aza-tricyclo[5.2.1.0 ^{2,6}]dec-8-ene-3,5-dione:	22
4.2 Synthesis of 2-Bromo-2-methyl-propionic acid 2-(3,5-dioxo-10-oxa-4-aza-tricyclo[5.2.1.0 ^{2,6}]dec-8en-4-yl)-ethyl ester (3).....	23
4.3 Synthesis of 2-Bromo-2-methyl-propionic acid 2-(2,5-dioxo-2,5-dihydro-pyrrol-1-yl)-ethyl ester (4).....	25
4.4 Synthesis of the BSA-macroiniator (5)	26
4.5 SET-LRP grafting of 2,2,2-trifluoroethyl acrylate (TFEA) from BSA-macroiniator 5 – Synthesis of BSA-poly(TFEA)	26
4.6 Photo-induced LRP grafting of 2,2,2-trifluoroethyl acrylate (TFEA) from BSA-macroiniator 5 – Synthesis of BSA-poly(TFEA).....	29
4.7 SET-LRP grafting of 2,2,2-trifluoroethyl methacrylate from BSA-macroiniator 5 – Synthesis of BSA-poly(TFEMA).....	32
4.8 Photo-induced LRP grafting of 2,2,2-trifluoroethyl methacrylate from BSA-macroiniator 5 – Synthesis of BSA-poly(TFEMA)	34
4.9 Photo-induced LRP grafting of 2,2,2-trifluoroethyl methacrylate from Ethyl α -bromoisobutyrate – Synthesis of ethyl-isobutyrate-poly(TFEMA).....	39
4.10 SET- LRP grafting of 2,2,3,3,4,4,5,5,6,6,7,7-Dodecafluoroheptyl acrylate (DFHA) from BSA- macroiniator 5 – Synthesis of BSA-poly(DFHA).....	42
4.11 Photo-induced LRP grafting of 2,2,3,3,4,4,5,5,6,6,7,7-Dodecafluoroheptyl acrylate (DFHA) from BSA- macroiniator 5 – Synthesis of BSA-poly(DFHA)	43

4.12 Grafting of styrene from BSA-macroinitiator 5 – Synthesis of BSA-PS following ATRP without applying any deoxygenation	46
Chapter 5: Conclusions	49
Chapter 6: Experimental Part	51
6.1. Materials.....	51
6.2. Analytical Methods	51
6.2.1. Nuclear magnetic resonance (NMR).....	51
6.2.2. Polyacrylamide gel Electrophoresis	52
6.2.3. Gel Permeation Chromatography (GPC)	52
6.2.4. Scanning Electron microscopy (SEM).....	52
6.3. Synthetic procedures	53
6.3.1 Synthesis of 4-(2-Hydroxyethyl)-10-oxa-4-aza-tricyclo[5.2.1.0 ^{2,6}]dec-8-ene-3,5-dione (2):.....	53
6.3.2 Synthesis of 2-Bromo-2-methyl-propionic acid 2-(3,5-dioxo-10-oxa-4-aza-tricyclo[5.2.1.0 ^{2,6}]dec-8en-4-yl)-ethyl ester (3).....	53
6.3.3 Synthesis of 2-Bromo-2-methyl-propionic acid 2-(2,5-dioxo-2,5-dihydro-pyrrol-1-yl)-ethyl ester (4).....	54
6.3.4 Synthesis of the BSA-macroiniator (5)	54
6.3.5 SET-LRP grafting of 2,2,2-trifluoroethyl acrylate (TFEA) from BSA-macroinitiator 5 – Synthesis of BSA-poly(TFEA).....	55
6.3.6 Photo-induced LRP grafting of 2,2,2-trifluoroethyl acrylate (TFEA) from BSA-macroinitiator 5 - BSA-poly(TFEA) – Synthesis of BSA-poly(TFEA)	55
6.3.7 SET-LRP grafting of 2,2,2-trifluoroethyl methacrylate from BSA-macroinitiator 5 – Synthesis of BSA-poly(TFEMA).....	56
6.3.8 Photo-induced LRP grafting of 2,2,2-trifluoroethyl methacrylate from BSA-macroinitiator 5 – Synthesis of BSA-poly(TFEMA)	57
6.3.9 Photo-induced LRP grafting of 2,2,2-trifluoroethyl methacrylate from Ethyl α -bromoisobutyrate – Synthesis of poly(TFEMA).....	58
6.3.10 SET- LRP grafting of 2,2,3,3,4,4,5,5,6,6,7,7-Dodecafluoroheptyl acrylate (DFHA) from BSA- macroinitiator 5 – Synthesis of BSA-poly(DFHA)	58
6.3.11 Photo-induced LRP grafting of 2,2,3,3,4,4,5,5,6,6,7,7-dodecafluoroheptyl acrylate (DFHA) from BSA- macroinitiator – Synthesis of BSA-poly(DFHA).....	59
6.3.12 ATRP grafting of styrene from BSA-macroinitiator 5 – Synthesis of BSA-polystyrene	60
Chapter 7: References	61

Chapter 1: Introduction

1.1 Fluorinated polymers

Fluorinated polymers (or fluoropolymers) are fluorocarbon-based polymers with multiple carbon–fluorine bonds. They possess a variety of useful chemical characteristics such as high resistance to solvents, acids, and bases. The most outstanding example of this family of polymers is polytetrafluoroethylene (Teflon) which was discovered by accident by Roy J. Plunkett, a recently hired Ph.D. at E.I. du Pont de Nemours and Company in 1938. The research interest on fluorine polymers is exponentially expanding as depicted in the number of papers per year on this scientific field according to Scopus (Figure 1).¹

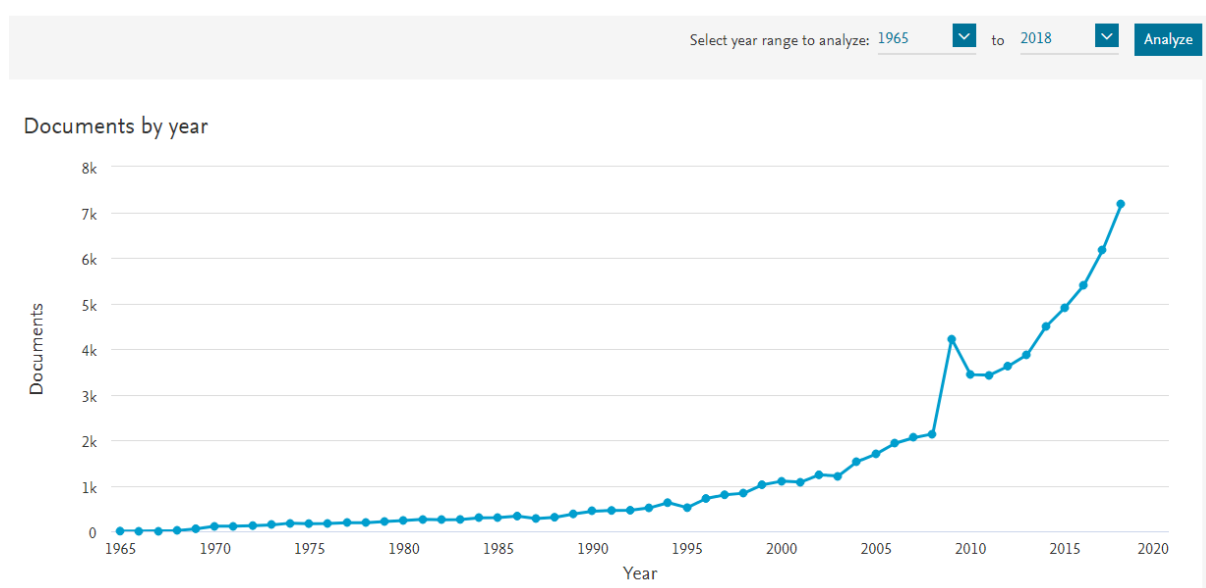


Figure 1: Number of papers per year on fluorinated polymers.¹

Fluoropolymers exhibit great inactivity to many chemicals and biological environments as well as hydrophobicity,² lipophilicity and self-healing ability³. Due to these properties fluoropolymers have been utilized in various biomedical applications such as ultrasound contrast agents, biosensors,⁴ protein storage,⁵ molecular imaging,⁶ prosthetics, fluorinated amphiphile-colloids, contact lens and drug delivery.⁷ Fluorinated molecules have many characteristics that can be attributed to the basic atomic properties of fluorine compared with those of other elements (Figure 2).⁸ The high ionization potential of fluorine indicate very weak intermolecular interactions, low surface energies, and low refractive indexes for perfluorocarbons. The extreme electronegativity of fluorine insures that it will always withdraw electron density when bonded to carbon, and these bonds will be strongly polarized, leading to C-F bonds with very high ionic character. Therefore, fluorinated materials can have

significant polar character as well. Also, the C-F bond is extremely strong and gets stronger and shorter as the number of fluorines that are bonded to the carbon increases (Figure 3).⁹

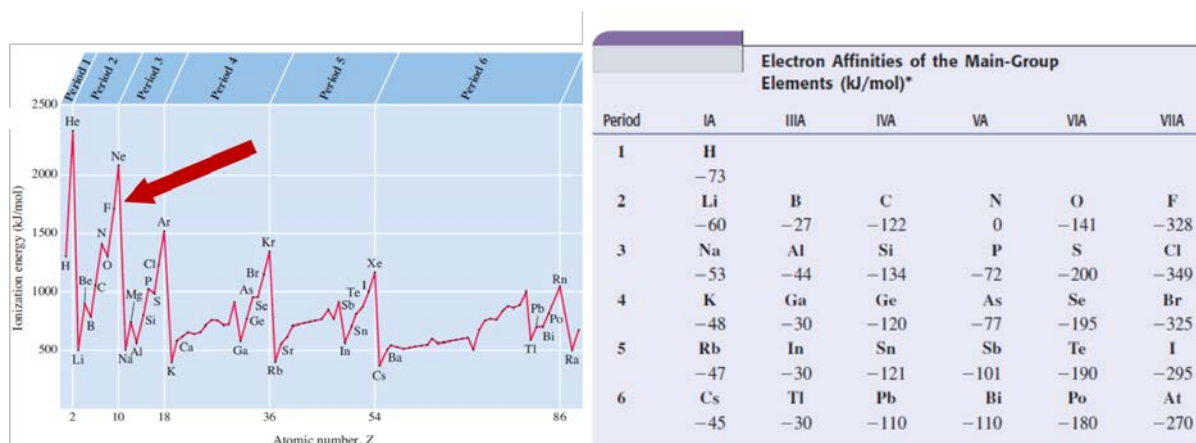


Figure 2: IP-ionization potential and EA-electron affinity of elements.⁸

TABLE I. * Bond lengths in fluorocarbons.

Compound ^{1,2}	Bond	Length (Å)	Difference(Å)
CH ₃ F	CF	1.391, 1.385	CF
			CC
CH ₂ F ₂	CF	1.358	0.030
			0.028
CHF ₃	CF	1.332, 1.326	0.010
CF ₄	CF	1.323	
CH ₂ =CH ₂	CC	1.337	
CH ₂ =CHF	CC	1.332	0.005
	CF	1.348	0.008
CHF=CHF	CC	1.324	0.011
	CF	1.337	0.004
CH ₂ =CF ₂	CC	1.320	0.016
	CF	1.321	0.007
CF ₂ =CF ₂	CC	1.313	0.008
	CF	1.313	

Figure 3: Bond lengths in fluorocarbons.⁹

1.2 Amphiphilic molecules

The word amphiphile comes from the Greek word “αμφίς” which means both and “φιλία” which means friendship, so an amphiphile is a chemical molecule that has affinity for two types of environments (two types of solvents). Amphiphilic molecules consist of a polar head group and a non-polar tail, which provide them affinity to polar and non-polar solvents at the same time (Figure 4). The polar head group is hydrophilic (water-loving) while the non-

polar tail is hydrophobic or lipophilic (fat-loving).¹⁰ The hydrophilic part is water-soluble and induces interactions of these molecules with aqueous solvents while the hydrophobic part is soluble in organic solvents making them interacting with non-aqueous media. Amphiphiles have the ability to form spherical micelles, vesicles¹¹, rod-like or spheroidal micelles, or even bilayer membranes. The concentration, the temperature, the pressure and the molecular structure are parameters that play a significant role concerning the type and the shape of the superstructures that will be formed by the amphiphilic molecules.¹²

Typical “small” amphiphilic molecules, have molecular weights on order of 500 Da, while “large” amphiphiles may have 10-1000 times larger molecular weights. Large amphiphiles are often created when a block of one type of a homopolymer attaches to another block, forming block copolymers with many useful properties. For example they can self-assemble into vesicles which can be utilized in drug delivery systems.¹³

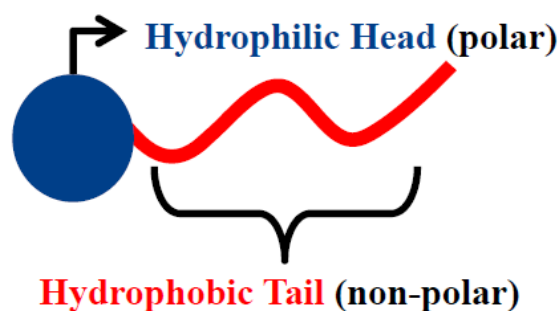


Figure 4: Structure of an amphiphilic molecule.

1.3 Giant Amphiphiles

Amphiphile molecules can be divided in three main categories depending on their molecular weight. Namely, there are molecular amphiphiles with low molecular weight (1kDa), super amphiphiles with intermediate molecular weight (6kDa) and giant amphiphiles with very high molecular weight (40kDa), (Figure 5).¹³ An example of low-molecular weight amphiphiles are the phospholipids which can aggregate into different supramolecular structures, determined by the shape of the molecule. Super amphiphiles are usually composed of amphiphilic diblock copolymers,¹⁴ which are molecules that contain both hydrophilic and hydrophobic polymeric blocks. Their aggregation pattern is mostly regulated from the block lengths or the presence of inorganic salts.^{13, 15}

The current thesis deals with the synthesis of giant amphiphiles, which are the largest, heaviest and latest discovered class of amphiphilic molecules. These molecules contain a polar head group consisting of an enzyme (or other protein), covalently connected to a non-

polar polymeric tail. The connection of these two parts usually is achieved by using a small linker molecule.^{10, 16} Giant amphiphiles have the ability to self-assemble into well-defined nanosized superstructures.¹⁷ The resulting morphologies remain analogous to those reported for lower molecular weight amphiphiles and are determined both from the shape and the length of the molecule. Noteworthy, giant amphiphiles combine the activity of the enzyme head-groups, which is often retained after the conjugation, with the extra properties of the hydrophobic polymeric tail. This characteristic opens new avenues in the development of nanosciences and increase the possible applications that such materials can find.

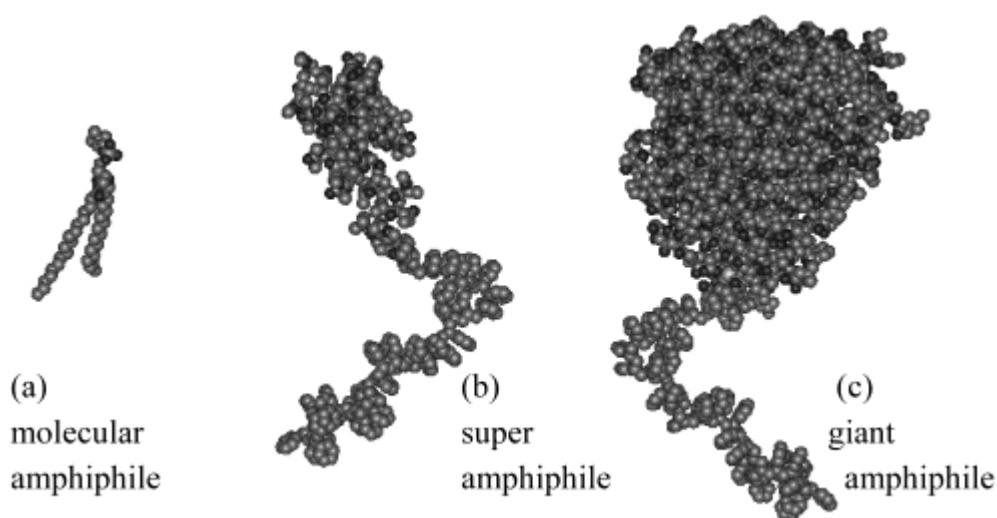


Figure 5: Models of (a) a molecular amphiphile with low molecular weight $\sim 1\text{kDa}$, (b) a super amphiphile with medium to high molecular weight $\sim 6\text{kDa}$, (c) a giant amphiphile with the highest molecular weight $\sim 40\text{kDa}$.¹³

There are three main approaches that these molecules can be synthesized, namely the “grafting to”, the “grafting from” and the “grafting through” methods. Following the grafting-to process, a polymer is firstly synthesized, purified and subsequently coupled to the biomolecule while in the grafting-from approach a small-molecule reactive handle is covalently attached to the biomolecule and used as an initiator to grow the polymeric chain from the surface of the protein. The grafting-through method involves the functionalization of monomers with a specific payload (Figure 6). The grafting-to method has been employed to a great extent due to the great advances that have been made in coupling chemistry and the utilization of versatile and efficient “click” reactions towards the generation of bioconjugates (Figure 6A). However, this method is accompanied by steric limitations during the coupling reaction and requires excess of the polymer. However, the grafting-from technique offers many advantages, especially regarding the purification of the prepared protein-polymer

bioconjugate.¹⁸ A representative example is reported in literature¹⁵ where the authors reported the first efficient ATRP-mediated in situ preparation of BSA-polystyrene giant amphiphiles in oxygen-free conditions and in the absence of cosolvent.

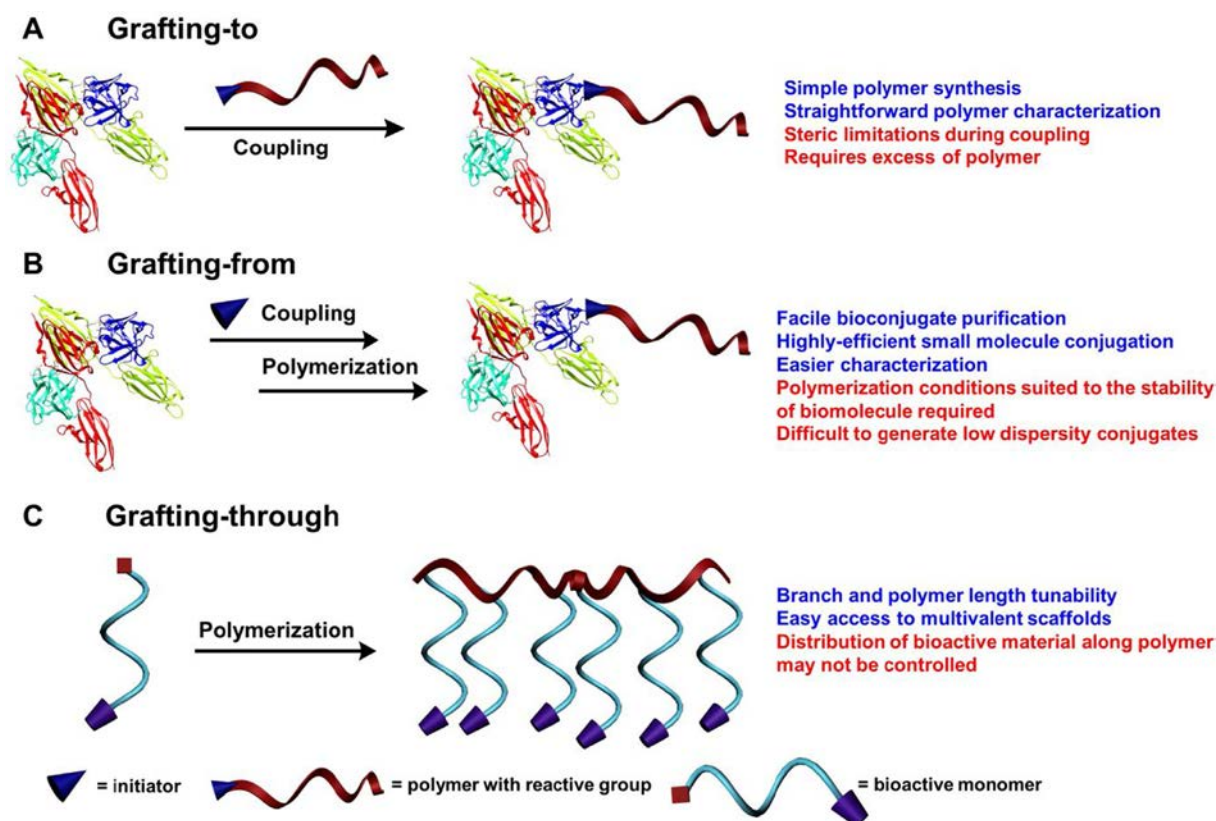


Figure 6. Schematic representations depicting different methods of preparing biomolecule-polymer conjugates along with a list of key advantages or disadvantages.^{18a}

1.4 Self-assembly

Molecular self-assembly is a well-established bottom up approach towards the creation of nano- and micro- materials with enhanced properties.¹⁹ There are two ways to construct nano- and micro- structures. The top-down approach begins from a bulk solid which is divided into smaller pieces until the formation of nano-sized materials. The bottom-up approach starts from molecules, which aggregate into clusters and finally form nano- and micro- materials. When the second procedure is reversible and proceeds in the absence of external forces, then it is defined as self-assembly.¹⁹ Self-assembly is characterized by the specific organization of the components as a result of intermolecular interactions.

Inspired by natural well-organized assemblies, chemists are investigating the molecular self-assembly of various building blocks to construct materials with improved properties. In the formation of large amphiphiles, the selection of the building blocks is

crucial, however another important challenge is to understand and dictate the cumulative non-covalent interactions that will participate throughout the formation of supramolecular structures. Such interactions are electrostatic and Van der Waals interactions, hydrogen bonds, π - π stacking, hydrophobic forces etc.²⁰

Because of their special structure, amphiphilic molecules are able to self-assemble into nano-structures depending on their surrounding environment. The driving force of this self-assembly process is the decrease in the free energy of the system as the non-soluble parts of the amphiphilic molecules try to reduce their contact with the environment (the solvent). A theoretical model was developed by the chemical engineer Jacob N. Israelachvili, which can predict the morphology of phospholipids depending on a packing parameter. From this formula, phospholipids with cone-shaped amphiphiles can self-assemble into spherical micelles in aqueous solutions, whereas cylindrical surfactants form vesicles. Moreover, when the size of the head group dominates the shape of the amphiphile, inverted micelles are formed (Figure 7).¹⁰








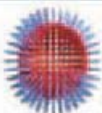
Aggregation Morphologies		
<i>Effective Shape of the Surfactant</i>	<i>Packing Parameter (P = v/al)</i>	<i>Aggregate Morphology</i>
 cone	$< 1/3$	 spherical micelles
 truncated cone	$1/3 - 1/2$	wormlike micelles 
 cylinder	$1/2 - 1$	bilayers, vesicles 
 inverted (truncated) cone	> 1	inverted micelles 

Figure 7: Various supramolecular configurations of molecular amphiphiles.¹⁰

1.5 ATRP (Atom Transfer Radical Polymerization)

In conventional free radical, anionic, or cationic polymerization, which is widely applied for the synthesis of million tons of polymers, the control of the polymer architecture and composition is very limited. Therefore, the advent of controlled living radical

polymerization (or controlled reversible-deactivation radical polymerization) has opened new avenues to the creation of advanced materials with precisely controlled molecular weight and narrow molecular weight distribution.²¹

Controlled radical polymerization (CRP) can be divided in three fundamental classes, namely there is Atom Transfer Radical Polymerization (ATRP), Reversible Addition/Fragmentation Chain Transfer Polymerization (RAFT) and Nitroxide-mediated Polymerization (NMP or SFRP). The increasing number of publications generally in CRP shows the importance of this area in polymer science (Figure 8). Among the most rapidly developed and widely used techniques, is Atom Transfer Radical Polymerization mediated by transition metal complexes, which provide a successfully controlled radical polymerization for the synthesis of well-defined polymers with an accurate and desirable architecture. It can be applied to a wide range of vinyl monomers acrylics, styrenes, acrylates, dienes and others.

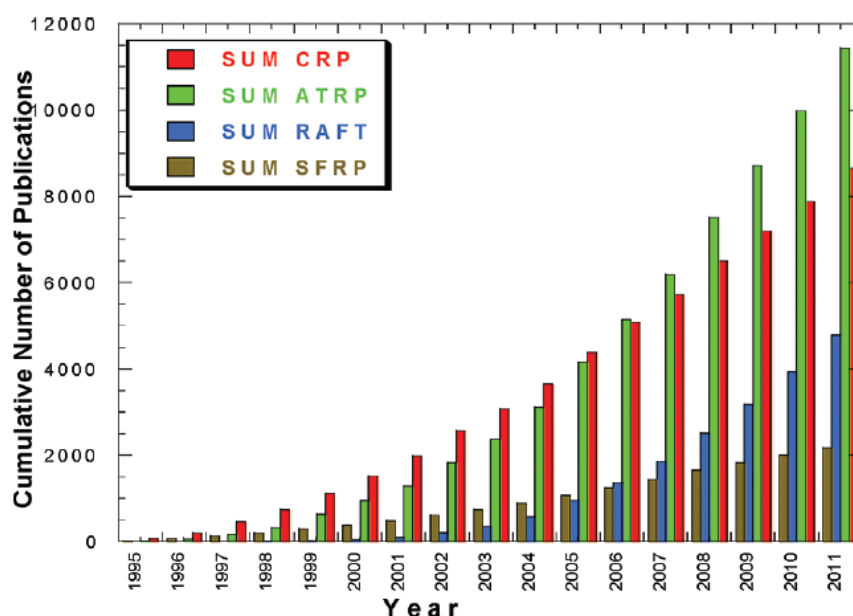


Figure 8: Number of publications on different Controlled Radical Polymerization methods according to SciFinder search on December 30, 2011.²¹

ATRP was developed in 1995 by Matyjaszewski and coworkers,²² in which an equilibrium is established through a reaction of a lower oxidized transition metal, e.g. Cu^{I} , and an alkyl halide. The transition metal is oxidized, e.g. Cu^{II} , and the radical can react reversely to form the alkyl halide.²³

The catalytic process of ATRP (Figure 9) begins with the abstraction of a halogen atom from an alkyl halide (R-X) by a transition metal catalyst (e.g. CuBr), which is oxidized (from $\text{Cu}^{\text{I}}\text{-X/L}$ to $\text{Cu}^{\text{II}}\text{-X/L}$). The scission of the alkyl-halide bond is homolytic, leaving a free radical which undergoes propagation, namely the newly created radicals continue reacting

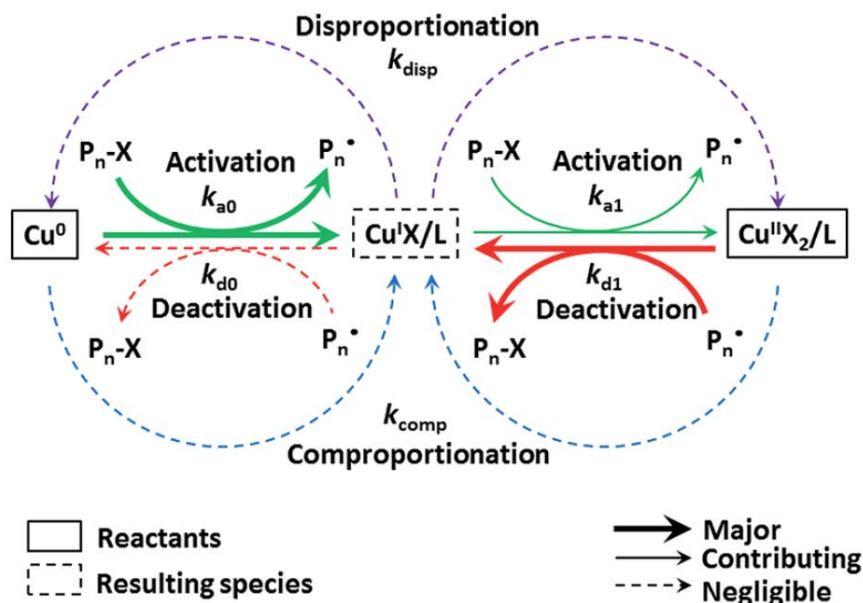


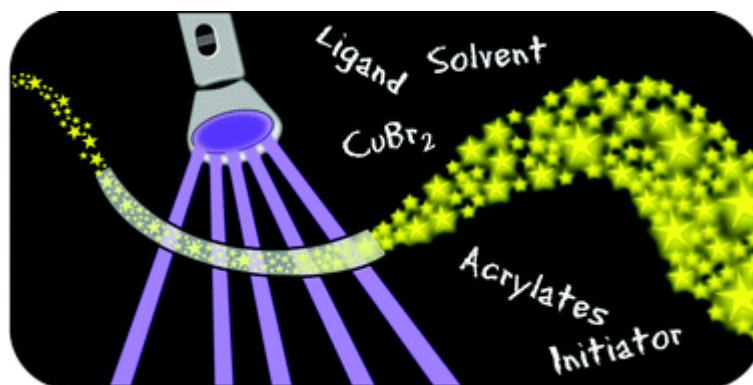
Figure 10: Proposed mechanism for SET-LRP.²³

As mentioned above the SET-LRP mechanism involves an equilibrium between P_n-X and $P_n\cdot$ (Figure 10) through a heterolytic outer sphere single electron-transfer process. Cu^0 or other electron-donor species, donate an electron to P_n-X resulting in an intermediate radical-anion $[P_n/P-X]^\cdot$, which degrades to $P_n\cdot$ and X^- . During the SET event or afterwards, the Cu^I species coordinate with a N-containing ligand. $Cu^I X/L$ complexes are rapidly disproportionated in coordinating solvents such as protic, dipolar aprotic, ionic liquids, and generally polar solvents, to generate extremely reactive atomic Cu^0 and $Cu^{II} X_2/L$ species. The $Cu^{II} X_2/L$ complex is capable to perform the reverse outer sphere oxidation of $P_n\cdot$ to P_n-X . This methodology facilitates an ultrafast Living Radical Polymerization of various activated monomers such as acrylates and methacrylates, and of nonactivated monomers containing electron-withdrawing groups such as vinyl chloride at room temperature.

1.7 Photo-induced Living Radical Polymerization

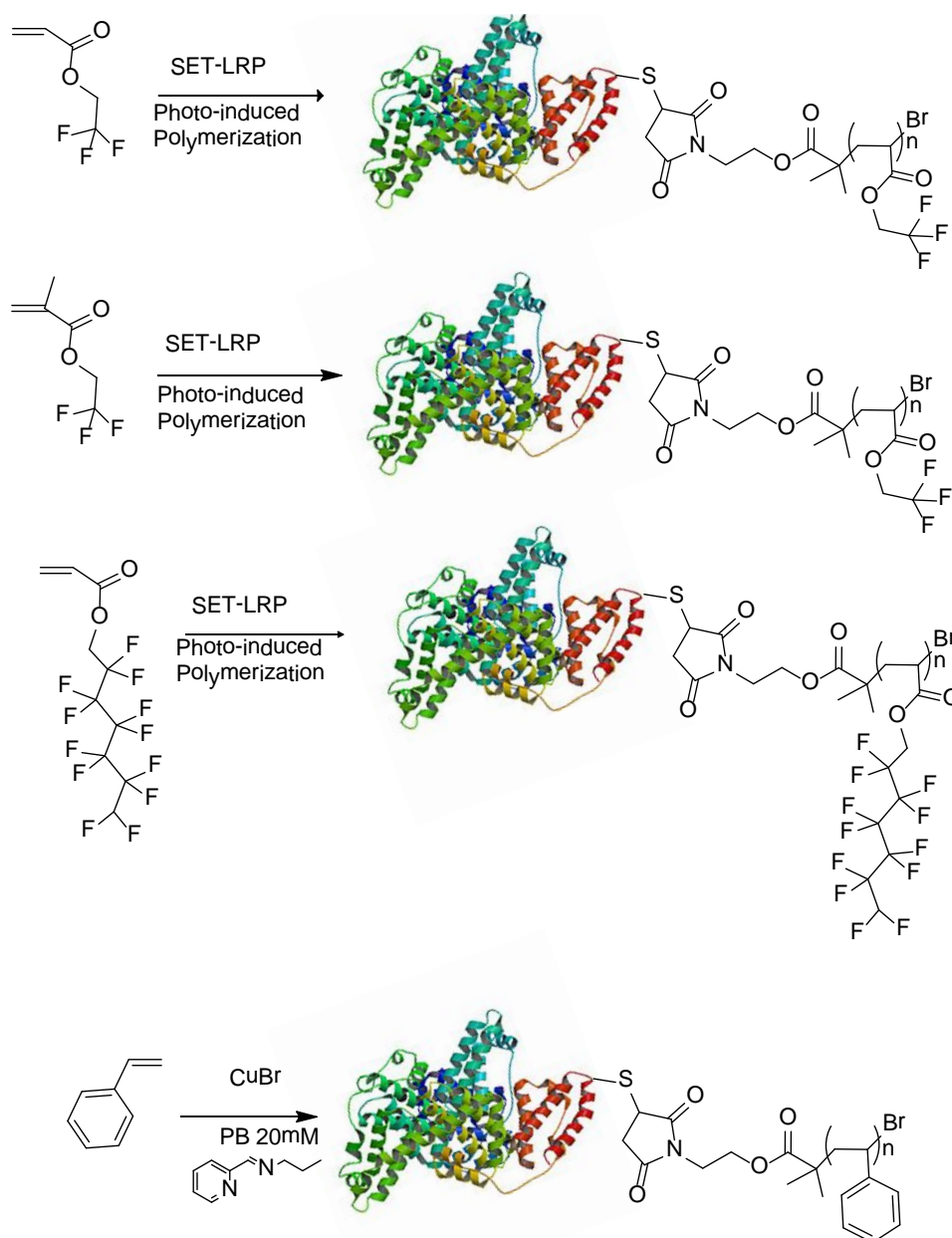
Recently a rather simple living polymerization technique has facilitated the synthesis of a variety of macromolecules utilizing low energy light source (LED) and a photoredox catalyst at ultralow concentrations. Photo-induced Living Radical Polymerization is a novel technique with encouraging results in the synthesis of polymers using a variety of monomers. Acrylates under a UV irradiation ($\lambda_{max} \sim 360$ nm) in the presence of an aliphatic tertiary amine ligand (Me_6TREN) and low concentrations of $CuBr_2$, can be efficiently converted into poly(acrylates) with barely any differences in their end-groups.^{18b}

The mechanism of photo-induced Living Radical Polymerization has been thoroughly investigated. The mechanism of photoRDRP has been recently examined via pulsed-laser polymerization (PLP) and high-resolution mass spectrometry which shown that it is a complex interaction between UV light and the typical reagents: ligand, initiator and Cu(II) bromide. In brief, the polymerization initiates via the UV light-induced scission of the alkyl–Br bond of the initiator, generating radicals that can propagate as well as react with copper(II) species that were present at the beginning. Subsequently, the Cu(I) species are generated through the electron transfer reaction between UV light-excited amine ligand species and the Cu(II) moieties. The excited Cu(II) complex is expected to be quenched by the free ligand producing the corresponding Cu(I) complex and the ligand becomes an amine radical cation. The role of the ligand is significant since it is the reducing agent of the reaction. However, there are other species able to promote the generation of Cu(I) species as well, such as alkyl and bromine radicals.²⁶ A recent example in literature showed that non-fluorinated, metal-free and visible light conditions can be also applied for the preparation of semifluorinated poly(meth)acrylates.²⁷



Chapter 2: Aims of the Thesis

The aim of this Bachelor thesis is the bioconjugation of a protein with perfluorinated polymers. More specifically, Bovine Serum Albumin (BSA) was used as a model protein and was conjugated with three fluorinated polymers and one non-fluorinated monomer, depicted in Scheme 1. To achieve this goal we applied two different synthetic approaches, namely SET-LRP and Photo-induced-LRP grafting of fluorinated monomers *from*²⁸ an bio-initiator. The classical procedures were altered through the use of syringe in order to limit the presence of the oxygen.

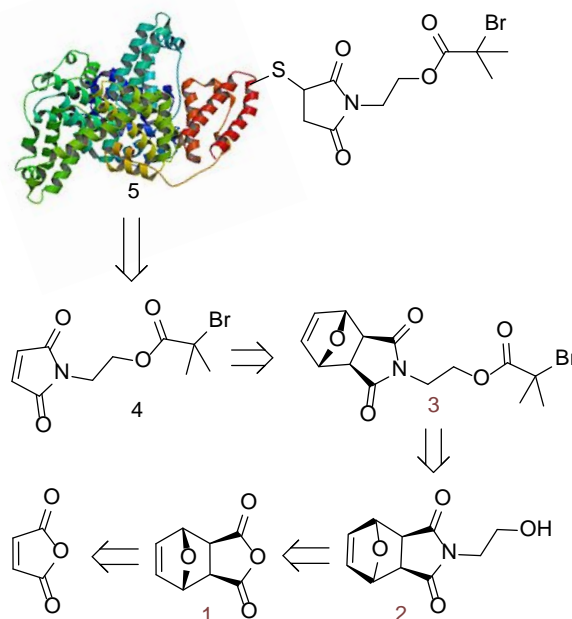


Scheme 1: Monomers and resulting protein polymer conjugates synthesized in the current thesis.

The synthesized protein polymer conjugates were fully characterized using various techniques such as PAGE electrophoresis, Gel Permeation Chromatography (GPC), Infrared Spectroscopy (IR), Scanning Electron Microscopy (SEM), $^1\text{H-NMR}$ and $^{19}\text{F-NMR}$ Spectroscopy. The three different fluorinated monomers that were investigated during the current thesis are 2,2,2-trifluoroethyl methacrylate, 2,2,2-trifluoroethyl acrylate, and 2,2,3,3,4,4,5,5,6,6,7,7-dodecafluoroheptyl acrylate along with, the non- fluorinated, styrene. Previous experimental studies were verified through our experimental approach.²⁹ Styrene was investigated with ATRP without the freeze pump thaw method in order to test whether it works and has acceptable yield.

The main target is the establishment of simpler synthetic protocols for the preparation of perfluorinated protein polymer conjugates and utilize $^{19}\text{F-NMR}$ for their characterization.

Chapter 3: Synthetic approaches

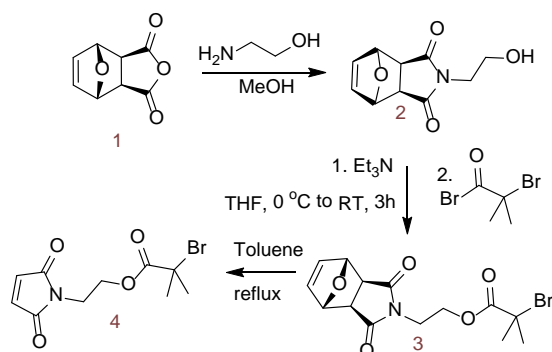


Scheme 2. Synthetic approach for the synthesis of the BSA-macroinitiator.

The synthetic route that can be followed for the preparation of the BSA-macroinitiator is illustrated in Scheme 2. Furan-2,5-dione can be converted into 3a,4,7,7a-tetrahydro-4,7-epoxyisobenzofuran-1,3-dione (anhydride 1) through a typical Diels–Alder reaction with furan. Ethanolamine can be used to convert anhydride 1 into 4-(2-hydroxyethyl)-10-oxa-4-aza-tricyclo[5.2.1.0^{2,6}]dec-8-ene-3,5-dione (alcohol 2). Esterification with the appropriate acyl bromide (2-bromo-2-methylpropanoyl bromide) can yield the maleimido-protected initiator 3. Retro-Diels–Alder reaction can afford the Maleimido-initiator 4, which subsequently can be coupled with the free thiol group of BSA, providing the desired BSA-macroinitiator 5.

Chapter 4: Results and Discussion

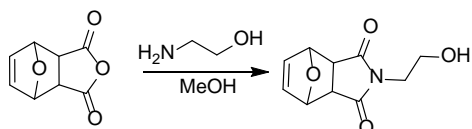
As mentioned above the aim of the current thesis is the growth of perfluorinated polymers chains from BSA utilizing SET-LRP and photo-induced-LRP (grafting *from* synthetic approach). In order to achieve this purpose, the synthesis of the initiator **4** which would be used in order to create the BSA-macroinitiator **5** was necessary. The corresponding steps of this synthesis are described below.



Scheme 3. Synthesis of the maleimido-initiator 4.

Maleimido-initiator **4** was synthesized twice during the current thesis as reported to literature.¹⁵ Since the anhydride **1** was already synthesized in the laboratory and enough amount was in stock, our experiments began with the synthesis of intermediate alcohol **2**.

4.1 Synthesis of 4-(2-Hydroxyethyl)-10-oxa-4-aza-tricyclo[5.2.1.0^{2,6}]dec-8-ene-3,5-dione:



Scheme 4. Synthesis of the alcohol 2.

Initially the anhydride **1** was suspended in MeOH (50 mL) and the mixture cooled to $0\text{ }^\circ\text{C}$. A solution of ethanolamine in MeOH was added dropwise in the reaction mixture which was stirred for 5 minutes at $0\text{ }^\circ\text{C}$. The mixture stirred at room temperature for 30 minutes and then reflux conditions were applied for 4 h. After cooling the mixture to ambient temperature, the solvent was evaporated under reduced pressure and the white residue was dissolved in CH_2Cl_2 and washed 3 times with of brine solution. The organic layer was dried over MgSO_4 , filtered and solvent was removed under reduced pressure providing a white-yellow residue. The TLC indicated



that the reaction was completed successfully since no initial anhydride was observed. The ^1H NMR spectrum of the clean product is depicted in Figure 11 and the peaks are fully assigned. Olefin protons 1 absorbs at 6.5 ppm while protons 2 are present in higher field. Aliphatic protons 4 and 5 absorbs at 3.70 and 3.75 ppm respectively. Protons 3 are the most shielded ones in this molecule.

Image 1. TLC plate of the obtained product.

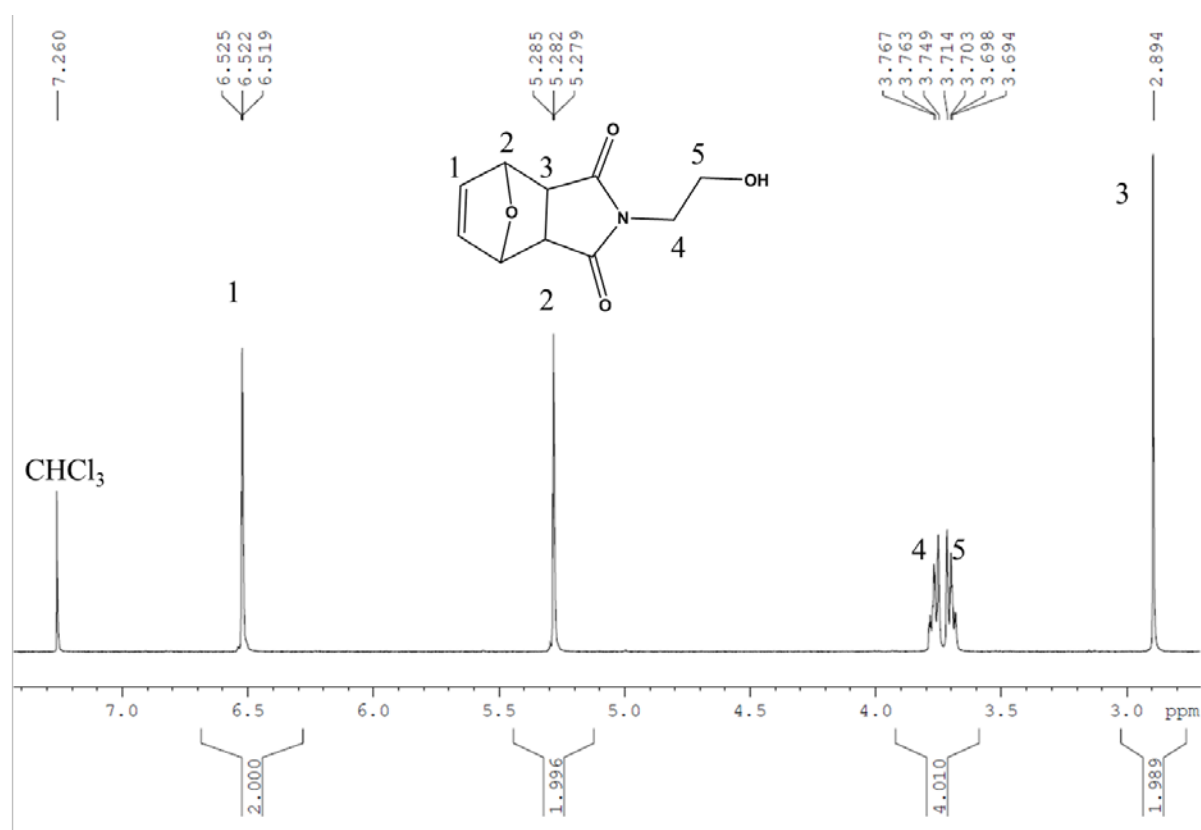
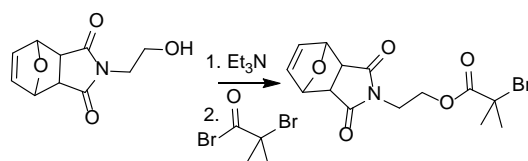


Figure 11. ^1H NMR Spectrum of alcohol 2 (500 MHz, CDCl_3 , 298 K): $\delta = \sim 1.90$ (bs, 1H, OH), 2.89 (s, 2H, CH), 3.69-3.71 (m, 2H, NCH_2), 3.75-3.78 (m, 2H, OCH_2), 5.28 (t, 2H, CH), 6.52 (t, 2H, CHvinyl).

4.2 Synthesis of 2-Bromo-2-methyl-propionic acid 2-(3,5-dioxo-10-oxa-4-azatricyclo[5.2.1.0^{2,6}]dec-8-en-4-yl)-ethyl ester (3)



Scheme 5. Synthesis of the maleimido-protected initiator 3.

In the next step the alcohol **2** was dissolved in THF and 1.2 equivalents of Et₃N was added. The slightly turbid mixture was cooled to 0 °C and a solution of 2-bromo-isobutyryl-bromide in THF was added dropwise. Afterwards the white suspension was stirred for 3 h at 0 °C and left overnight at room temperature. TLC (P.E.:AcOEt) revealed the formation of the desired product. The ammonium salt byproduct was filtered off and the solvent removed under reduced pressure to give a pale-yellow residue.

In order to obtain the clean maleimido-protected initiator **3**, a column chromatography with SiO₂ gel and petroleum ether/ethyl-acetate at 1:1 ratio solvent eluent was conducted to give the pale-yellow product **3**. The reaction was monitored by TLC revealing that the maleimido-protected initiator **3** was eluted in fractions 24-38. These fractions were combined and the solvent was removed under reduced pressure, yielding to product **3**.



Image 2. TLC plates of the fractions eluted during the chromatographic purification of the product **3**.

The ¹H NMR spectrum of the clean product is depicted in Figure 12 and the peaks are fully assigned. Olefin protons (**1**) absorb at 6.5 ppm while protons (**2**) are present in higher field. Aliphatic protons **4** and **5** absorb at 4.32 and 3.81 ppm respectively. They are shifted to lower field compared to the corresponding peaks of alcohol **2**. Aliphatic protons (**6**) are the most protected ones in this molecule.

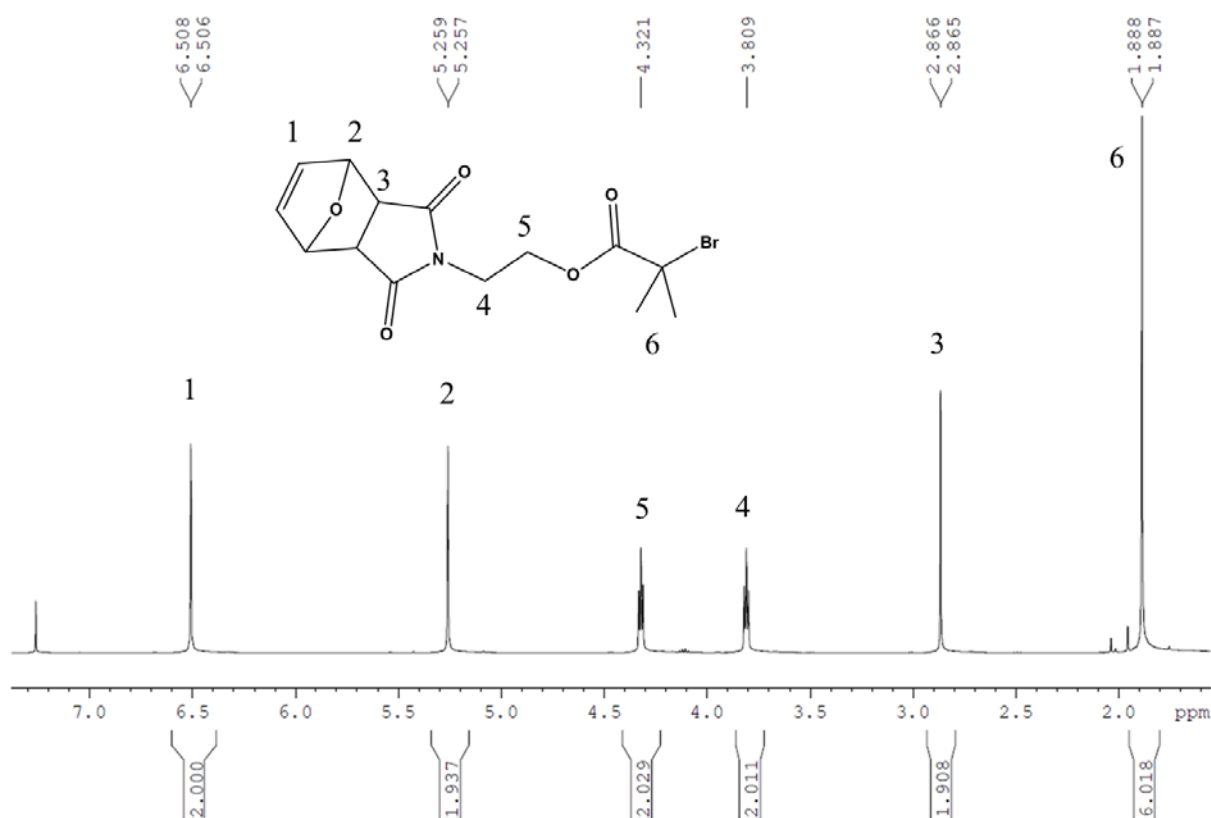
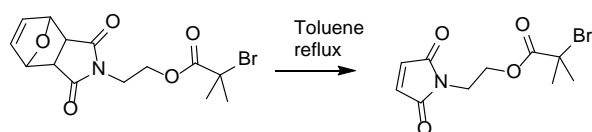


Figure 12. ^1H NMR Spectrum of maleimido-protected initiator 3 (500 MHz, CDCl_3 , 298 K): $\delta = 1.89$ (bs, 6H, CH_3), 2.86 (s, 2H, CH), 3.81 (t, 2H, NCH_2), 4.32 (t, 2H, OCH_2), 5.26 (m, 2H, CHO), 6.51 (m, 2H, CHvinyl).

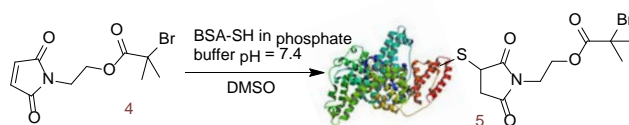
4.3 Synthesis of 2-Bromo-2-methyl-propionic acid 2-(2,5-dioxo-2,5-dihydro-pyrrol-1-yl)-ethyl ester (4)



Scheme 6. Synthesis of the maleimido-initiator 4.

A solution of the maleimido-protected initiator 3 was suspended in toluene and reflux conditions were applied under nitrogen atmosphere overnight. Finally, the solvent was removed under reduced pressure to give the maleimido-initiator 4.

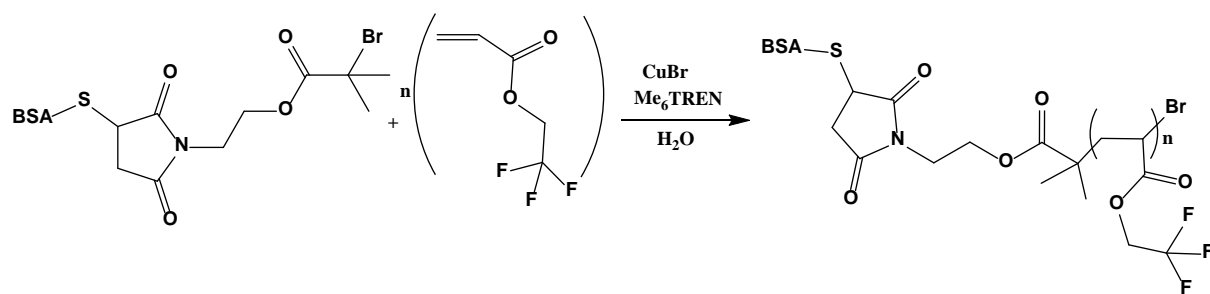
4.4 Synthesis of the BSA-macroinitiator (5)



Scheme 7. Synthesis of BSA- macroinitiator 5.

The preparation of the macromolecular bio-initiator begins with a solution of the maleimido-initiator **4** in DMSO which was slowly added in a solution of BSA in 20 mM phosphate buffer (pH 7.4). The reaction mixture was gently shaken for about 48 hours at ambient temperature. In order to eliminate the excess of the initiator **4**, the mixture was extensively dialyzed: once against 5 mM phosphate buffer pH 7.4 and 10% MeCN for 48 hours and then once against 5 mM phosphate buffer pH 7.4 (using regenerated cellulose dialysis membranes with a MWCO of 25 kDa) for 2 hours and finally once against 20 mM phosphate buffer pH 7.4 for another 2 hours. After that, the solution of the BSA macroinitiator **5** was centrifuged, was freeze dried and stored at $-20\text{ }^{\circ}\text{C}$. In Figure 13 the lane 1 corresponds to the band of the BSA macroinitiator **5** and lane 2 depicts the BSA protein.

4.5 SET-LRP grafting of 2,2,2-trifluoroethyl acrylate (TFEA) from BSA-macroinitiator 5 – Synthesis of BSA-poly(TFEA)



Scheme 8. Synthesis of BSA-poly(TFEA).

After the synthesis of bioinitiator **5**, next step was to graft fluorinated monomers for the creation of new bioconjugates with BSA. 2,2,2-trifluoroethyl acrylate monomer was chosen for the first polymerization reaction using the SET-LRP grafting method.

For this purpose, the amount of CuBr (40 equiv.) and Tris[2-(dimethylamino)ethyl]amine (Me_6TREN) (40 equiv.) were dissolved in H_2O and placed in a plastic syringe. The mixture was left under gentle stirring at $0\text{ }^{\circ}\text{C}$ for 3 minutes for the activation of the copper catalyst. The reaction mixture becomes blue while black solid particles appear which correspond to

Cu⁰. Subsequently BSA-macroinitiator **5** (1 equiv.) and 2,2,2-trifluoroethyl acrylate monomer (2000 equiv.) were introduced to the mixture in the syringe and the reaction was stirred overnight at room temperature. The headspace of the syringe was eliminated in order to get rid of the undissolved oxygen from the reaction mixture.

In order to eliminate the excess of monomer and other low molecular weight reagents (such as the ligand and copper), the mixture was extensively dialyzed against 5 mM phosphate buffer 7.4, 10% MeCN and EDTA overnight, then against 5 mM phosphate buffer 7.4 for 2 hours and finally against 20 mM phosphate buffer 7.4 for 2 hours carried out. Regenerated cellulose dialysis membranes with MWCO 25 kDa were used for dialysis.

The formation of the desired bioconjugate was verified by native PAGE (Figure 13). The appearance of new dark blue bands in the well of the stacking gel slightly migrating within the stacking gel combined with the absence of the band corresponding to the reactant biomacroinitiator **5** verified the quantitative formation of the bioconjugate.

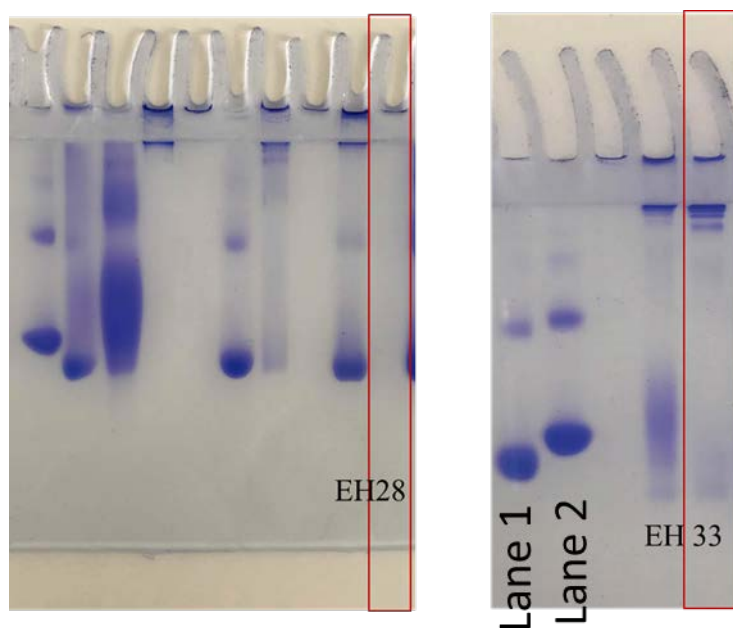


Figure 13. Electrophoretic behavior of BSA-poly(TFEA) synthesized in two independent reactions.

What is more, the formation of the bioconjugate was further supported by GPC chromatography (Figure 14). The GPC chromatograms showed that in both reactions (leading to products EH28 and EH33) the polymerization was successful due to the faster elution of the bioconjugates when compared to the elution of the bioinitiator under the same conditions, indicating the formation of a product with larger hydrodynamic diameter.

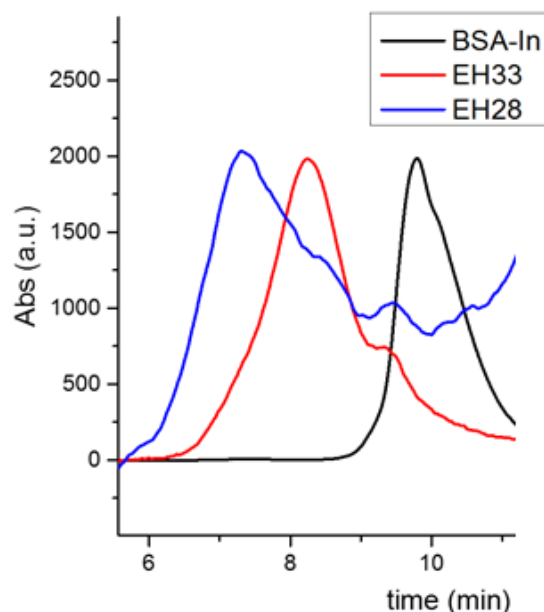


Figure 14. GPC Spectrum of the BSA-macroinitiator **5** (BSA-In) and BSA-poly(TFEA) from two independent reactions.

The product was also analyzed with ^{19}F -NMR in D_2O (Figure 16) and compared with the spectrum of the monomer (Figure 15). The monomer NMR spectrum contains two peaks at -73.7 (triplet) and -75.7 (broad). This could be attributed to the interaction between Fluorine atoms and the aqueous solvent (D_2O). In the case of the protein polymer bioconjugate the new peak appearing at -74.9 ppm indicates the formation of the BSA-poly(TFEA).

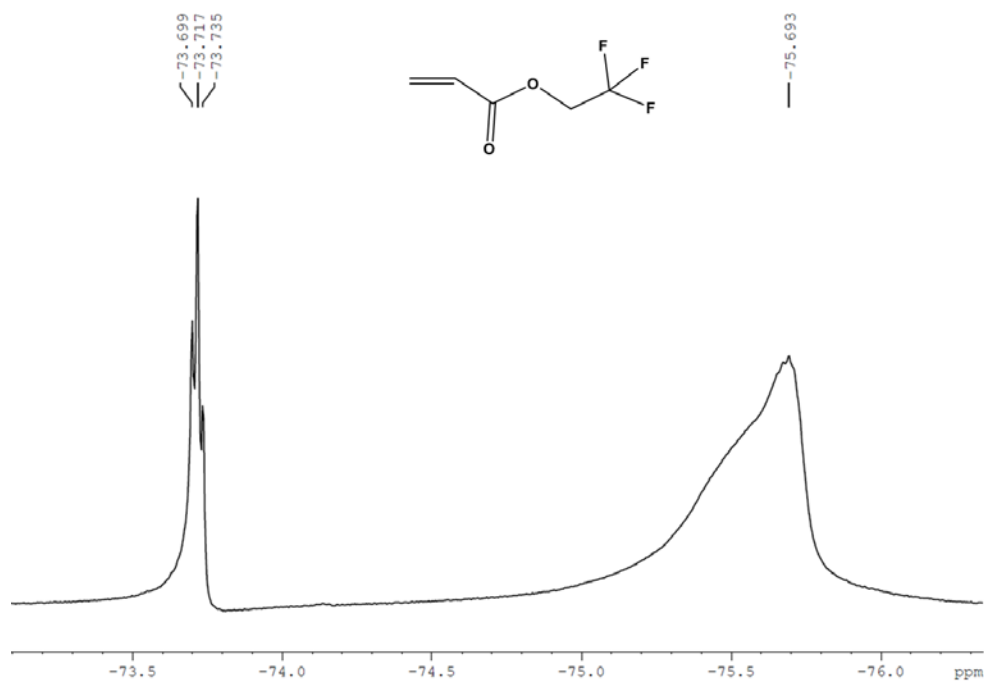


Figure 15. ^{19}F NMR Spectrum of 2,2,2-trifluoroethyl acrylate monomer (500 MHz, D_2O , 298 K): $\delta = -73.72$ (m, 3F, CF_3), -75.69 (bs).

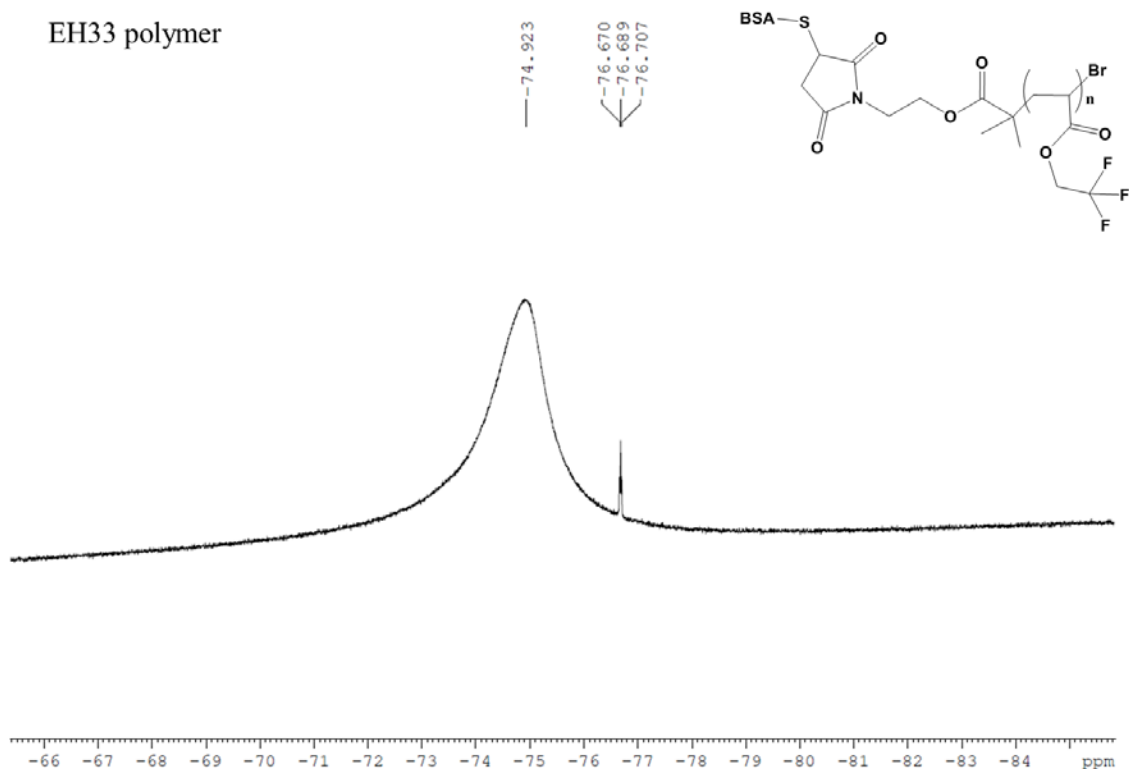
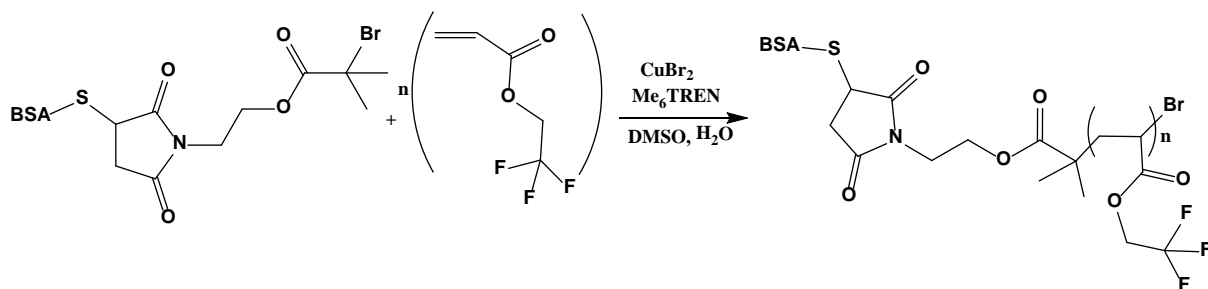


Figure 16. ^{19}F NMR Spectrum of BSA-poly(TFEA) polymer (500 MHz, D_2O , 298 K): $\delta = -74.92$ (bs), -76.69 (m).

4.6 Photo-induced LRP grafting of 2,2,2-trifluoroethyl acrylate (TFEA) from BSA-macroinitiator 5 – Synthesis of BSA-poly(TFEA)



Scheme 9. Synthesis of BSA-poly(TFEA).

Subsequently we performed the same synthesis following the photo-induced LRP instead. For this purpose a solution of BSA-macroinitiator **5** (1.25 ml, 1 equiv.) and a stirrer were placed in a milliliter syringe. Then the monomer 2,2,2-trifluoroethyl acrylate (TFEA) (0.11 ml, 0.874 mmol, 2000 equiv.) was dissolved in a mixture of 0.29 ml water and 0.2 ml DMSO. A solution of Me_6TREN (14 μl , 0.0524 mmol, 120 equiv) and CuBr_2 (1.5 mg, 0.00655 mmol, 15 equiv) in 1 ml of nanopure water was also prepared. Firstly, the monomer solution was added to the initiator solution using a glass pipette. Finally, 100 μl of the aqueous solution

containing CuBr_2 and Me_6TREN were quickly added and air was removed. A light blue color was immediately observed and great care was given in order to avoid air bubbles and the headspace was eliminated. The syringe was fitted with a rubber septum, placed under a UV nail lamp (365 nm), and the reaction mixture was left under stirring, for about 8 hours.

In order to eliminate the excess of monomer and other low molecular weight reagents (such as the ligand and copper), the mixture was extensively dialyzed initially against 5 mM phosphate buffer 7.4, 10% MeCN and EDTA overnight, another one dialysis against 5 mM phosphate buffer 7.4 for 2 hours and finally against 20 mM phosphate buffer 7.4 for 2 hours. After the purification, the product was studied with PAGE-electrophoresis (Figure 17). The appearance of new dark blue bands in the well of the stacking gel slightly migrating within the stacking gel combined with the absence of the band of the biomacroinitiator **5** proved that the reaction was quantitative.

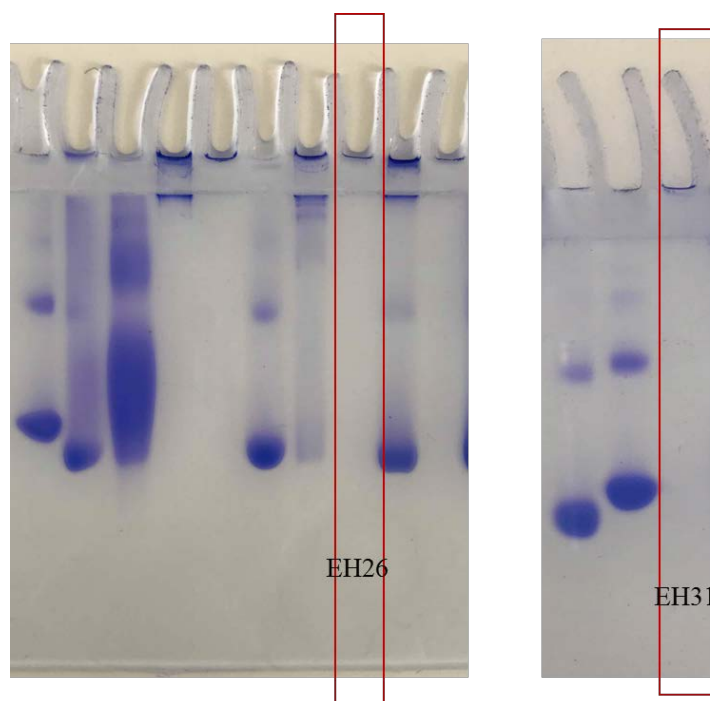


Figure 17. Electrophoretic behavior of BSA-poly(TFEA) synthesized in two independent reactions

Furthermore, the formation of the bioconjugate was also supported by GPC chromatography (Figure 18). The GPC chromatograms showed that in both reactions (leading to products EH26 and EH31) the polymerization was successful due to the faster elution of the bioconjugates when compared to the elution of the bioinitiator under the same conditions, indicating their larger hydrodynamic diameter.

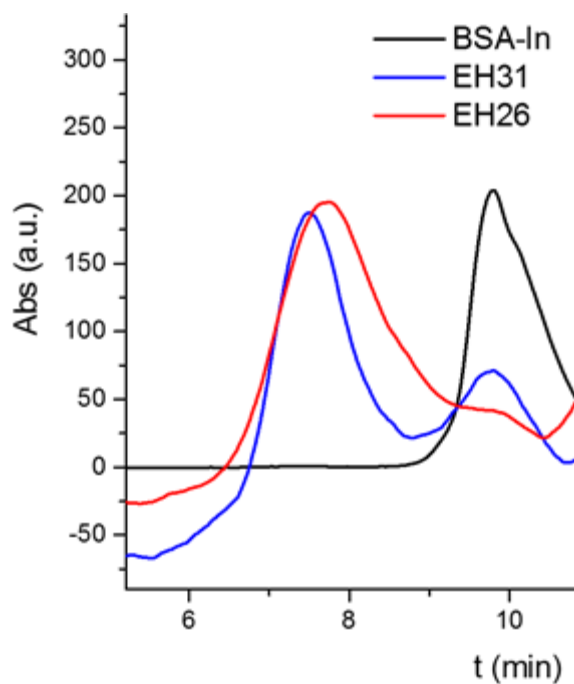


Figure 18. GPC Spectrum of BSA-macroinitiator 5 (BSA-In) and bioconjugate BSA-poly(TFEA) from two independent reactions.

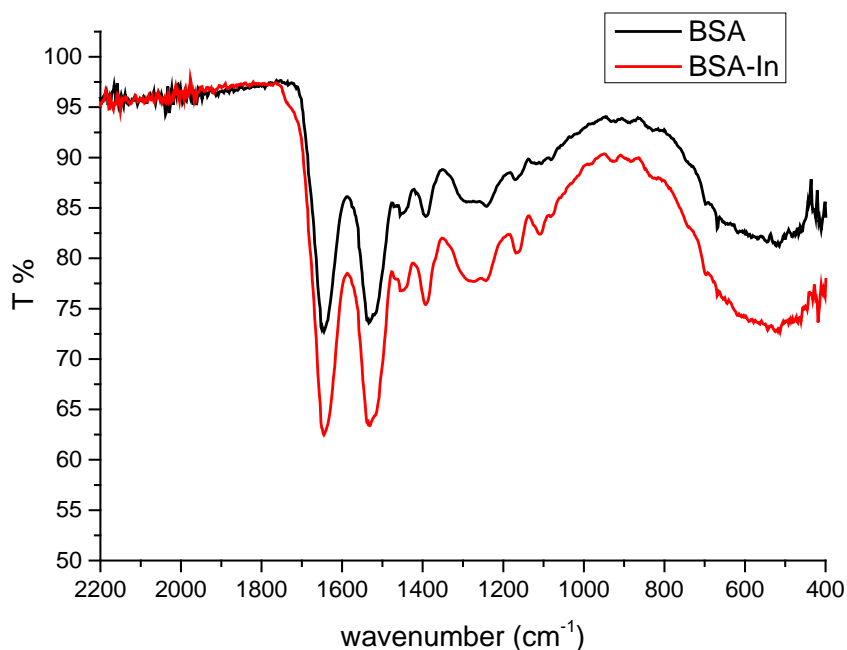


Figure 19. IR Spectrum of BSA protein and BSA-In.

As shown in Figure 19 there is no significant change at the IR spectrum of BSA and BSA-In. The product was also analyzed with FTIR spectroscopy (Figure 20) and compared to the corresponding spectrum of BSA protein and BSA-In. The new peak appearing at 1276 cm^{-1} indicates the successful formation of the polymer because it is characteristic for the vibration of the C-F bonds.

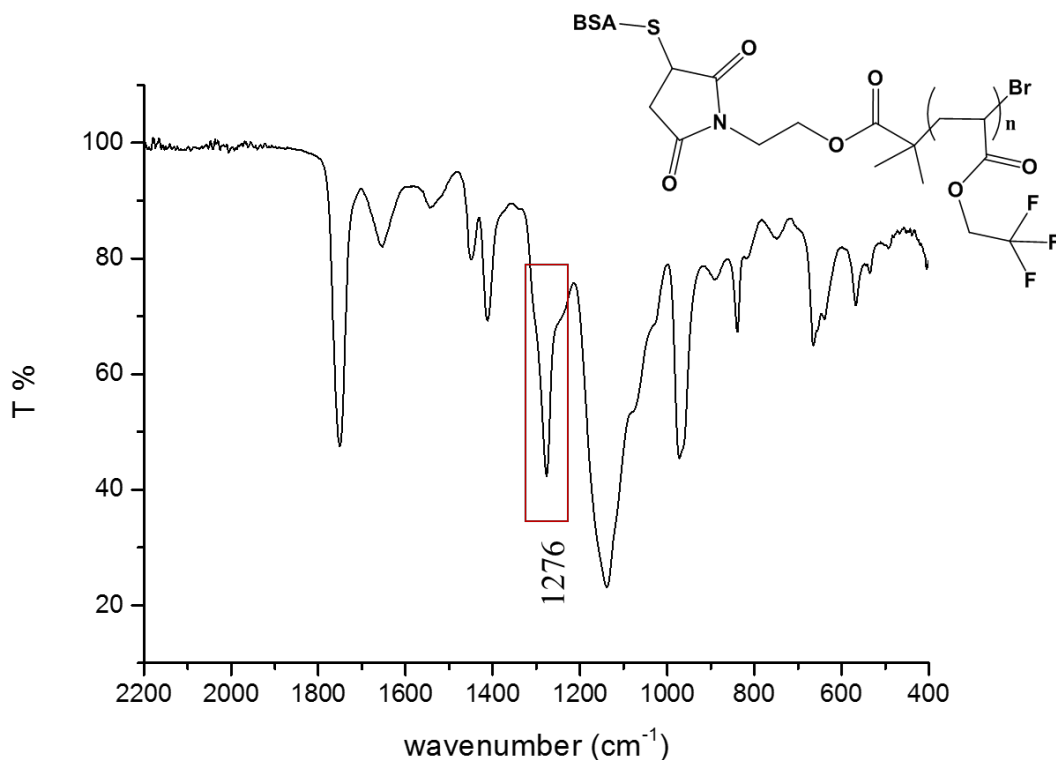
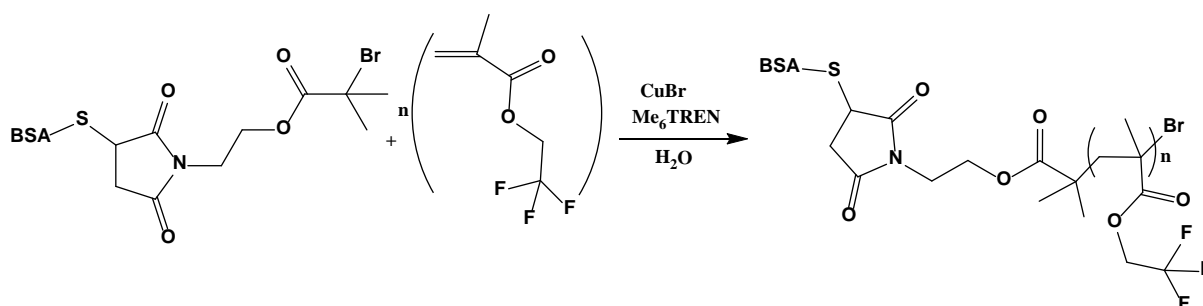


Figure 20. IR Spectrum of BSA-poly(TFEA).

4.7 SET-LRP grafting of 2,2,2-trifluoroethyl methacrylate from BSA-macroinitiator **5** – Synthesis of BSA-poly(TFEMA)



Scheme 10. Synthesis of BSA-poly(TFEMA).

We proceeded the synthesis using another fluorine monomer, the 2,2,2-trifluoroethyl methacrylate. Firstly the amounts of CuBr (40 equiv.) and Tris[2-(dimethylamino)ethyl]amine (Me₆TREN) (40 equiv.) were dissolved in 0.37 mL H₂O and placed in a plastic syringe. The mixture was stirred gently at 0 °C for 3 minutes for the activation of the copper catalyst. After that BSA-macroinitiator **5** (1 equiv.) and 2,2,2-trifluoroethyl methacrylate monomer (2000 equiv.) were introduced to the mixture in the syringe and the reaction was left stirring overnight at room temperature. The use of the syringe eliminated the headspace of the reaction by pushing the plunge of the syringe so only

the dissolved oxygen remains in the reaction mixture. The crude polymerization mixture was purified using dialysis initially against 5 mM phosphate buffer 7.4, 10% MeCN and EDTA overnight, then against 5 mM phosphate buffer 7.4 for 2 hours and finally against 20 mM phosphate buffer 7.4 for 2 hours carried out. Regenerated cellulose dialysis membranes with MWCO 25 kDa were used for dialysis.

After the purification, the product was studied with PAGE-electrophoresis (Figure 21). The appearance of new dark blue bands in the well of the stacking gel slightly migrating within the stacking gel show the formation of the polymer product but the band of the biomacroinitiator **5** is also present indicating that the reaction was not successful.

Moreover, the formation of the bioconjugate was also supported by GPC chromatography (Figure 22). The GPC chromatograms showed that the EH27 experiment lead to significant polymerization since there is a band appearing at shorter elution times. However the presence of some amount of biomacroinitiator **5** is further supported since its characteristic band under the same conditions is also observed, proving that the consumption of the BSA-macroinitiator was partial.

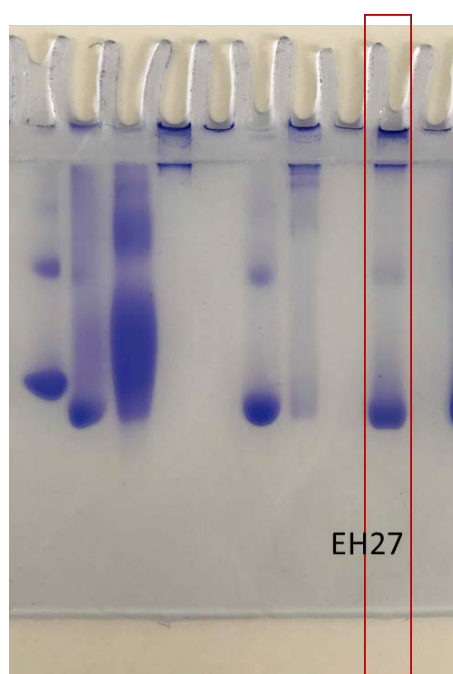


Figure 21. Electrophoretic behavior of BSA-poly(TFEMA).

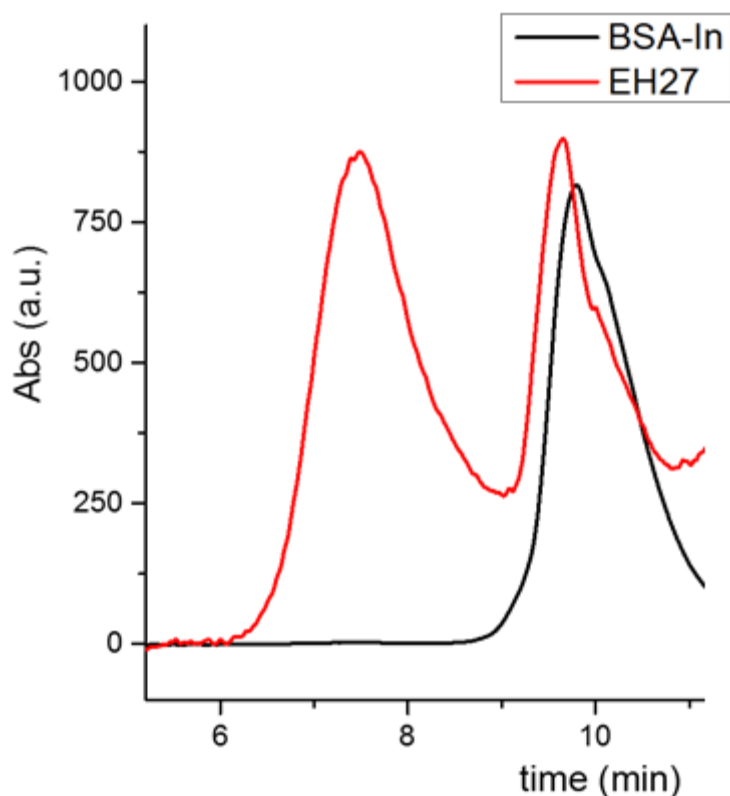
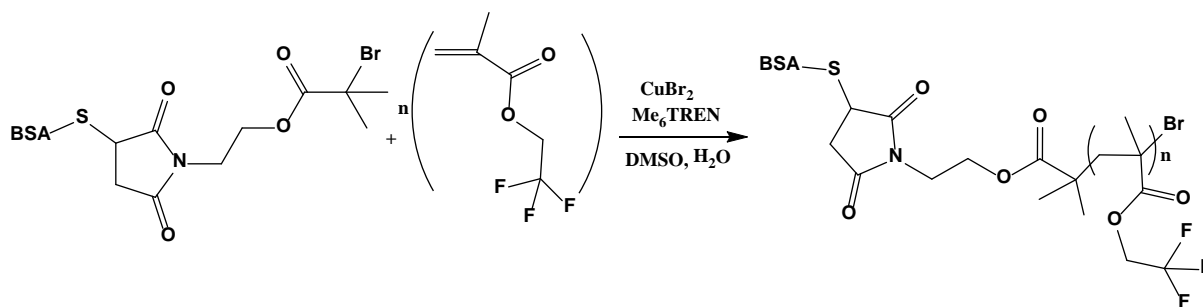


Figure 22. GPC spectrum of the BSA-macroinitiator **5** (BSA-In) and bioconjugate BSA-poly(TFEMA).

4.8 Photo-induced LRP grafting of 2,2,2-trifluoroethyl methacrylate from BSA-macroinitiator **5** – Synthesis of BSA-poly(TFEMA)



Scheme 11. Synthesis of BSA-poly(TFEMA).

We also performed the same synthesis following the photo-induced LRP grafting method. For this purpose a solution of BSA-macroinitiator **5** (1 equiv.) and a stirrer were placed in a milliliter syringe. Then the monomer 2,2,2-trifluoroethyl methacrylate (TFEMA) (2000 equiv.) was dissolved in a mixture of 0.3 ml water and 0.2 ml DMSO. A solution of Me₆TREN (120 equiv) and CuBr₂ (15 equiv) in 1 ml of nanopure water was also prepared. Firstly, the monomer solution was added to the initiator solution using a glass pipette. Finally,

100 μ l of the aqueous solution containing CuBr_2 and Me_6TREN were quickly added and air was removed. A light blue color was immediately observed and great care was given in order to avoid air bubbles and eliminate the reaction headspace. The syringe was fitted with a rubber septum, placed under a UV nail lamp (365 nm), and the reaction mixture was left under stirring, for about 6 hours.

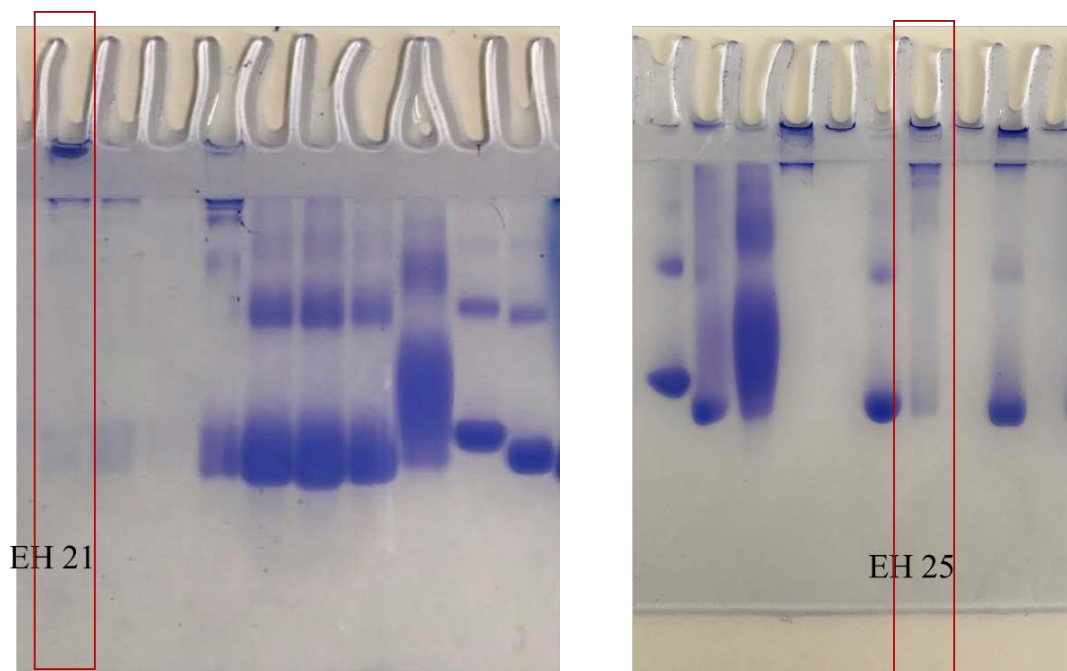


Figure 23. Electrophoretic behavior of BSA-poly(TFEMA) synthesized in two independent reactions.

In order to eliminate the excess of monomer and other low molecular weight reagents (such as the ligand and copper), the mixture was extensively dialyzed initially against 5 mM phosphate buffer 7.4, 10% MeCN and EDTA overnight, another one dialysis against 5 mM phosphate buffer 7.4 for 2 hours and finally against 20 mM phosphate buffer 7.4 for 2 hours. After the purification, the product was studied with PAGE-electrophoresis (Figure 23). The appearance of new dark blue bands in the well of the stacking gel slightly migrating within the stacking gel combined with the absence of the band of the biomacroinitiator **5** proved that the reaction was quantitative.

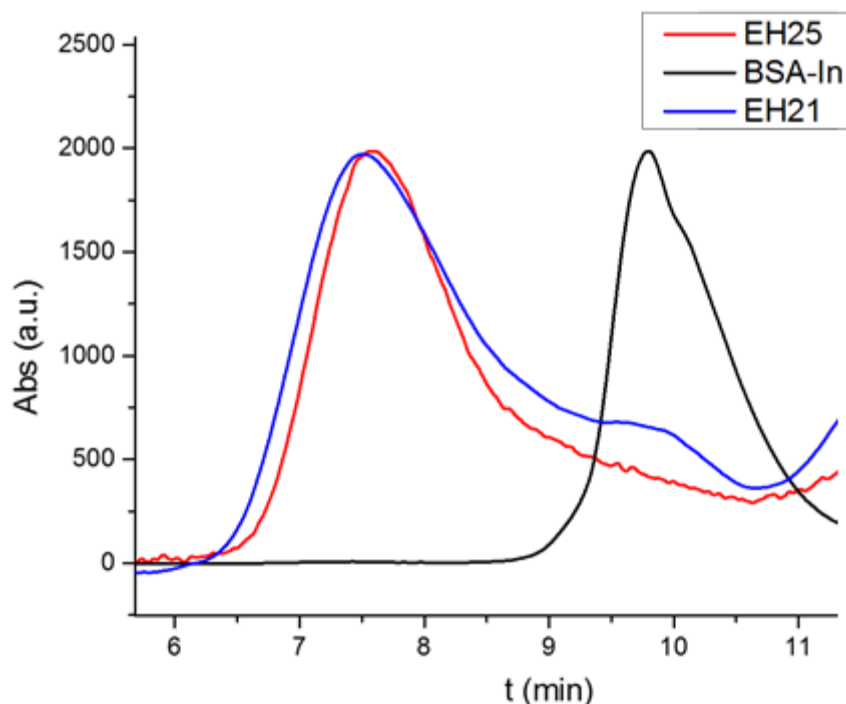


Figure 24. GPC Spectrum of BSA-macroinitiator 5 (BSA-In) and bioconjugate BSA-poly(TFEMA) from two independent reactions.

What is more, the formation of the bioconjugate was also supported by GPC chromatography (Figure 24). The GPC chromatograms showed that in both reactions (leading to products EH21 and E25) the polymerization was successful due to the faster elution of the bioconjugates when compared to the elution of the bioinitiator under the same conditions, indicating that they do have higher molecular weight.

Finally the product was analyzed with ^{19}F -NMR in D_2O (Figure 26) and compared with the spectrum of the monomer (Figure 25). The monomer NMR spectrum contains two peaks at -73.8 (triplet) and -75.77 (broad) as the previous one. As it was mentioned before this can be attributed to the interaction between Fluorine atoms and the aqueous solvent (D_2O). The new peak in the spectrum of the protein polymer bioconjugate appearing at -74.1 ppm indicates the formation of the BSA-poly(TFEMA).

From the above one can conclude that the photo-induced LRP grafting was proven to be more efficient in the case of this particular bioconjugate.

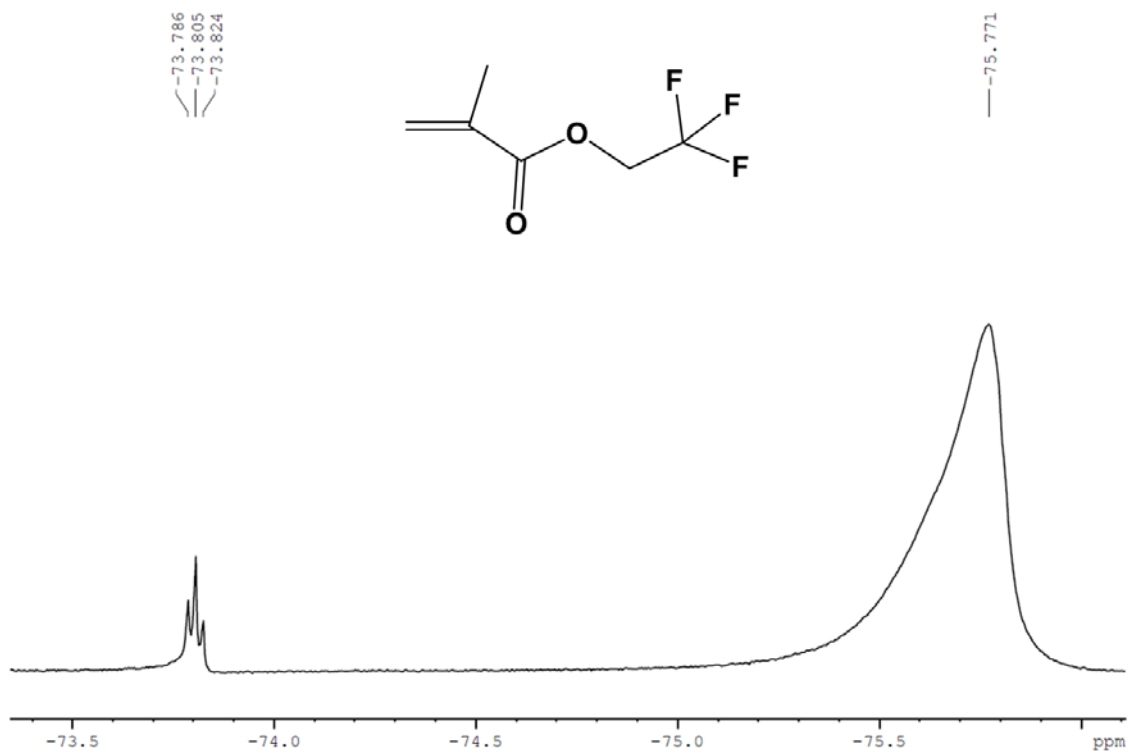


Figure 25. ^{19}F NMR Spectrum of 2,2,2-trifluoroethyl methacrylate monomer (500 MHz, D_2O , 298 K): $\delta = -73.80$ (m, 3F, CF_3), -75.77 (bs).

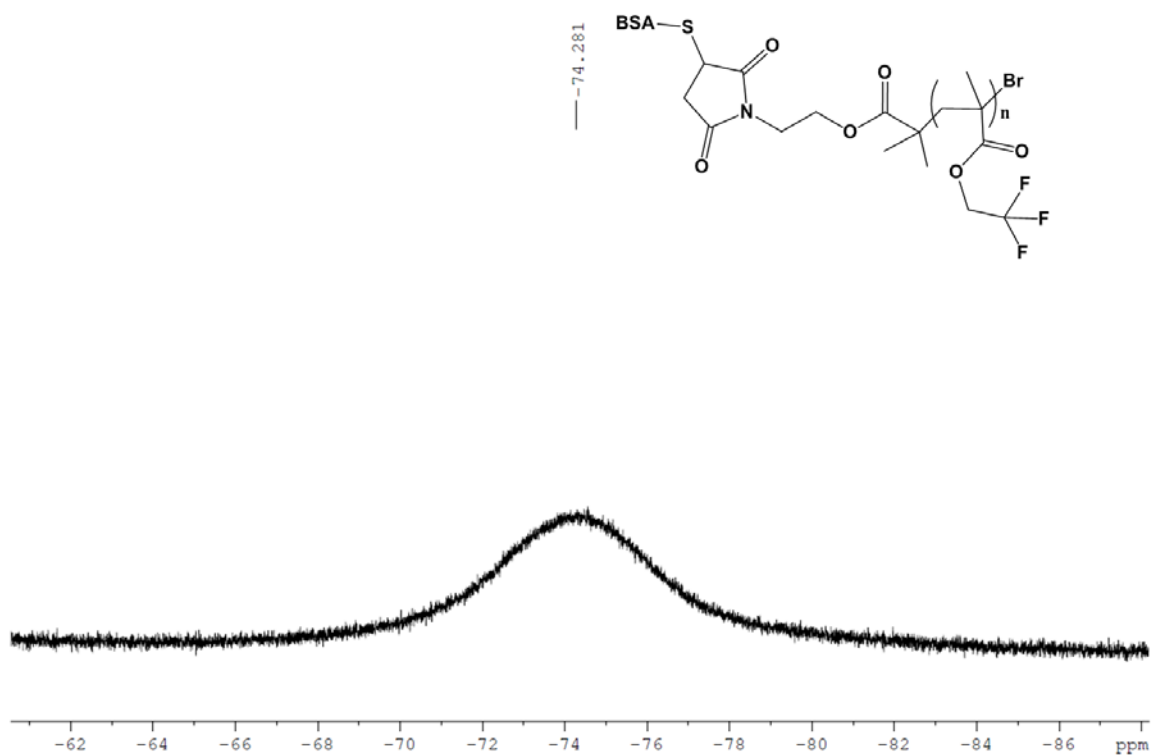


Figure 26. ^{19}F NMR Spectrum of BSA-poly(TFEMA) polymer (500 MHz, D_2O , 298 K): $\delta = -74.28$ (bs).

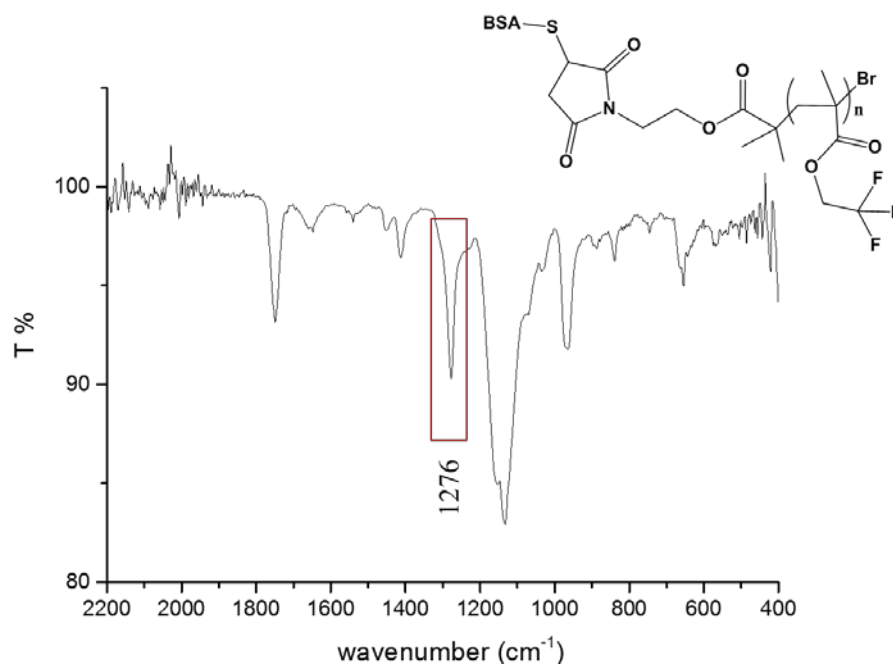


Figure 27. IR Spectrum of BSA-poly(TFEMA).

The BSA-poly(TFEMA) polymer was also analyzed with FTIR spectroscopy (Figure 27) where the peak appearing at 1276 cm^{-1} , which is attributed to the stretching vibration of the ester group (C=O) indicates the successful formation of the polymer. At 1450 cm^{-1} the bending vibration peak of $-\text{CH}_2-$ appears and at 1385 cm^{-1} the flexural vibration peak of C-H in $-\text{CH}_3$ is also observed. The absorption bands corresponding to the stretching vibration of C-F are depicted around 1236 cm^{-1} . Moreover at 1143 cm^{-1} the stretching vibration peak of C-H was found. A series of absorption bands associated with the C-O bond at 841 cm^{-1} were identified. As well as the absorption peak at 754 cm^{-1} is assigned to the stretching vibration of C-F.

Furthermore, the self-assembling ability of this product was investigated through scanning electron microscopy (Figure 28) which revealed that this protein-polymer conjugate is able to self-assemble into spherical nanostructures of $\sim 0.2\text{ }\mu\text{m}$ diameter, due to its amphiphilic character.

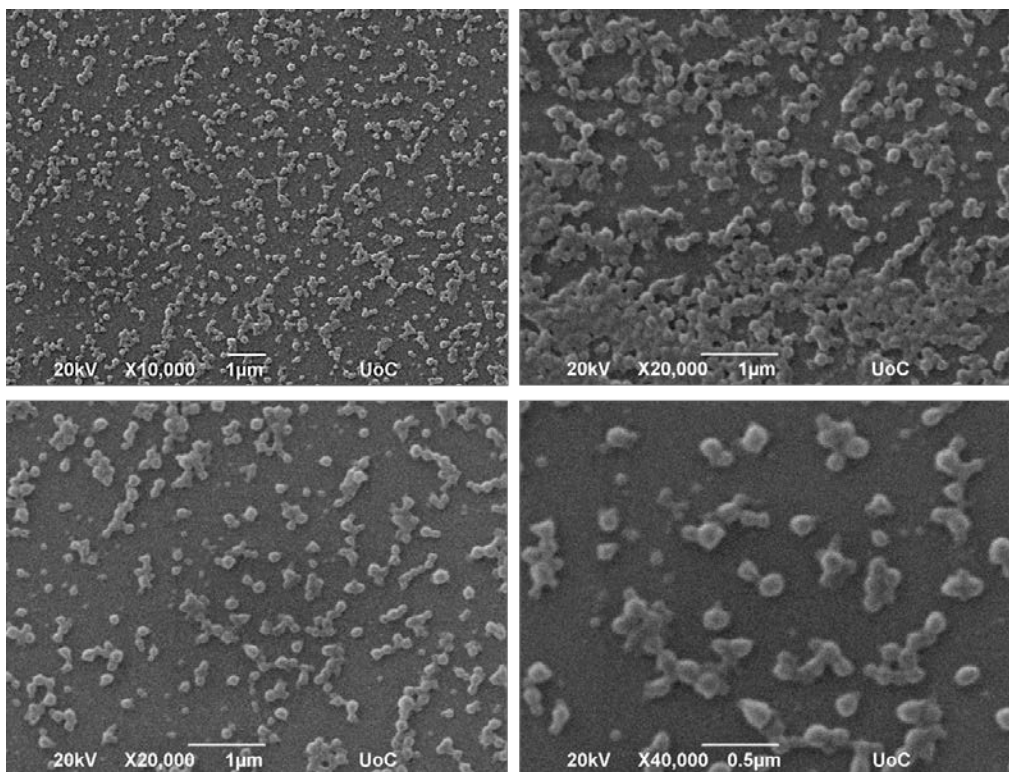
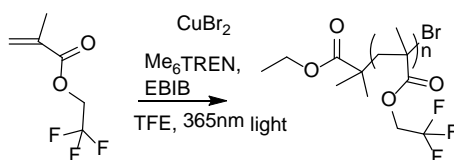


Figure 28. SEM images of BSA-poly(TFEMA).

4.9 Photo-induced LRP grafting of 2,2,2-trifluoroethyl methacrylate from Ethyl α -bromoisobutyrate – Synthesis of ethyl-isobutyrate-poly(TFEMA)



Scheme 12. Synthesis of ethyl-isobutyrate-poly(TFEMA).

Continuing our studies we selected the 2,2,2-trifluoroethyl methacrylate monomer in order to create a fluorinated polymer without a protein bio-initiator. For this goal 2,2,2-trifluoroethyl methacrylate monomer (50 equiv.) was added to a rubber septum-sealed vial equipped with a stirring magnet. Then, a solution of Me₆TREN (0.12 equiv) and CuBr₂ (0.02 equiv) in 35 μ l TFE was added to the vial followed by EBIB (1 eq). The reaction mixture was purged with nitrogen for 10 min and placed under a UV lamp (365 nm) for 8h.

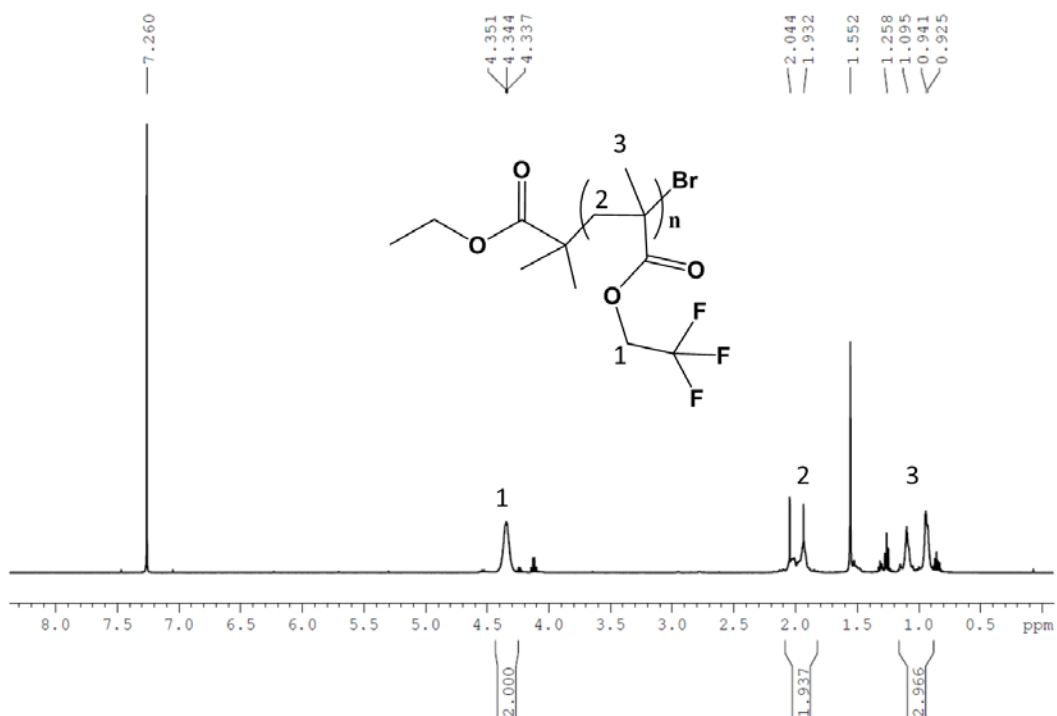


Figure 29. ¹H NMR Spectrum of ethyl-isobutyrate-poly(TFEMA).

The polymer product was analyzed with ¹H and ¹⁹F-NMR (Figures 29, 30). The peaks of the polymer in the ¹H NMR were fully assigned as depicted in the above figure. By comparing the ¹⁹F-NMR of the polymer (Figures 30) with the corresponding spectrum of the monomer (Figure 25) with the polymer, the new peak appearing at -73.3 ppm indicates the successful formation of ethyl-isobutyrate-poly(TFEMA). Comparing this peak with the corresponding one of the BSA-poly(TFEMA) bio-polymer, the biopolymer appears at one ppm lower ppm (-74.3) (Figure 26). More significantly the peak of the polymer is more sharp than the broad peak of the biopolymer and this is an expected behavior due to the aggregation (self-assembly) caused by the protein.

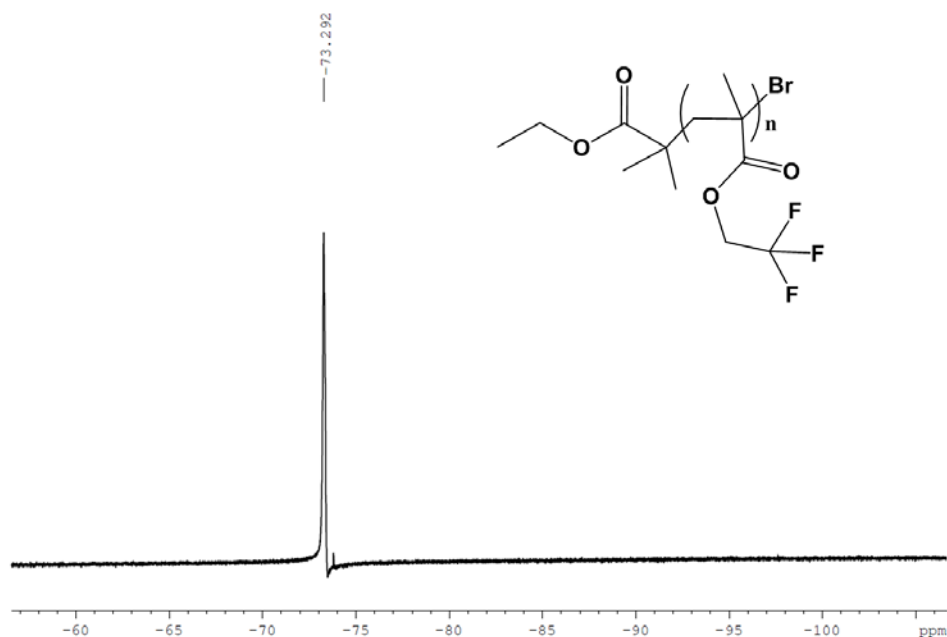


Figure 30. ^{19}F NMR Spectrum of ethyl-isobutyrate-poly(TFEMA).

In Figure 31 the FTIR spectra of BSA-macroinitiator **5** (BSA-In), of bio-conjugate BSA-poly(TFEMA) and of ethyl-isobutyrate-poly(TFEMA) are presented. Both the Bio-polymer and the polymer exhibit a peak at 1276 cm^{-1} while the initiator does not. This observation is representative for the successful formation of the corresponding polymers.

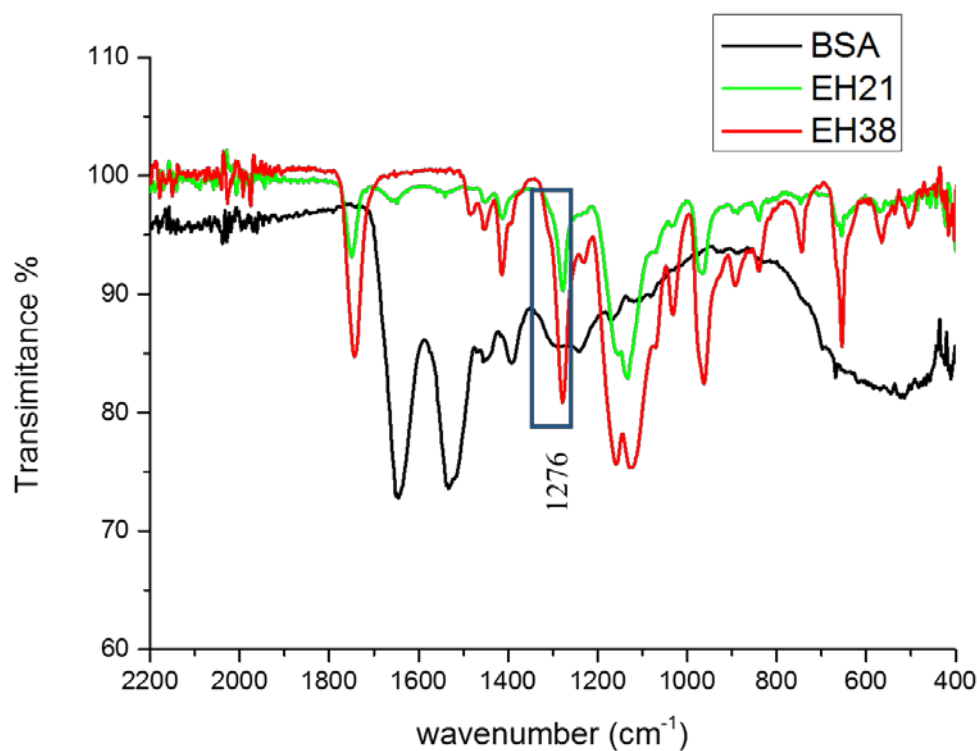
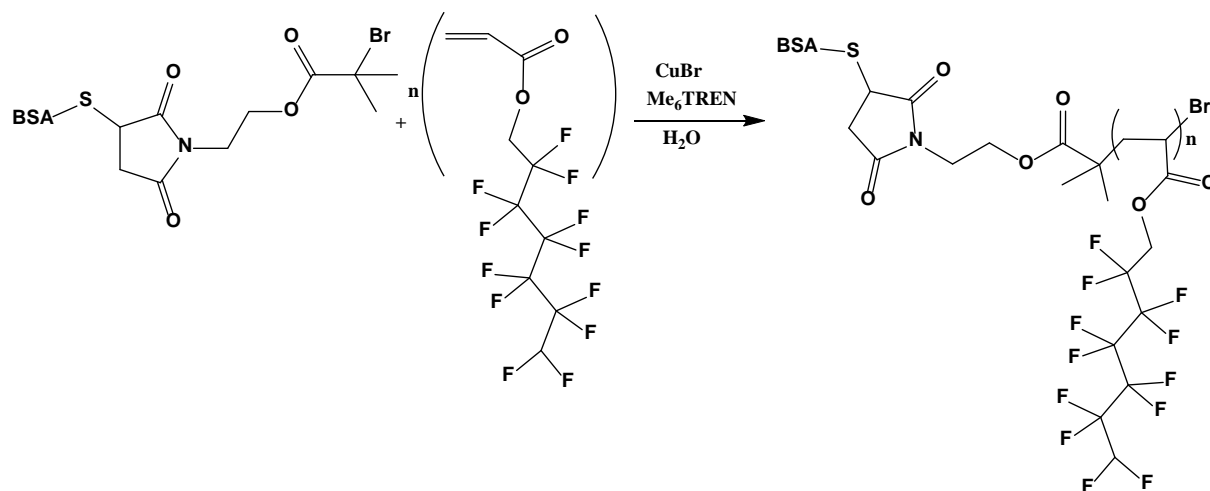


Figure 31. IR spectra of BSA-initiator **5**, bio-conjugate BSA-poly(TFEMA) and ethyl-isobutyrate-poly(TFEMA).

4.10 SET- LRP grafting of 2,2,3,3,4,4,5,5,6,6,7,7-Dodecafluoroheptyl acrylate (DFHA) from BSA- macroinitiator **5** – Synthesis of BSA-poly(DFHA)



Scheme 13. Synthesis of BSA-poly(DFHA).

Another monomer that was part of our investigations is 2,2,3,3,4,4,5,5,6,6,7,7-Dodecafluoroheptyl acrylate. For the synthesis of the corresponding biopolymer, initially the amount of CuBr (40 equiv.) and Tris[2-(dimethylamino)ethyl]amine (Me₆TREN) (40 equiv.) were dissolved in 0.37 mL deionized H₂O and placed in a plastic syringe. The mixture was let under gentle stirring at 0 °C for 3 minutes for the activation of the copper catalyst. Subsequently BSA-macroinitiator **5** (1 equiv.) and the monomer 2,2,3,3,4,4,5,5,6,6,7,7-dodecafluoroheptyl acrylate (2000 equiv.) were introduced to the mixture in the syringe and the reaction was stirred overnight at room temperature.

In order to eliminate the excess of monomer and other low molecular weight reagents (such as the ligand and copper), the mixture was extensively dialyzed against 5 mM phosphate buffer 7.4, 10% MeCN and EDTA overnight, then against 5 mM phosphate buffer 7.4 for 2 hours and finally against 20 mM phosphate buffer 7.4 for 2 hours carried out. Regenerated cellulose dialysis membranes with MWCO 25 kDa were used for dialysis.

After the purification, the product was studied with PAGE-electrophoresis (Figure 32). The appearance of new dark blue bands in the well of the stacking gel slightly migrating within the stacking gel show formation of some amount of polymer product but the band of the biomacroinitiator **5** is also present indicating that the reaction was not successful. The density of the bands indicate low yield of polymerization.

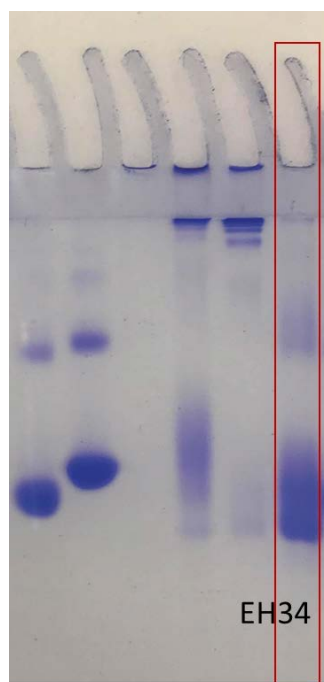
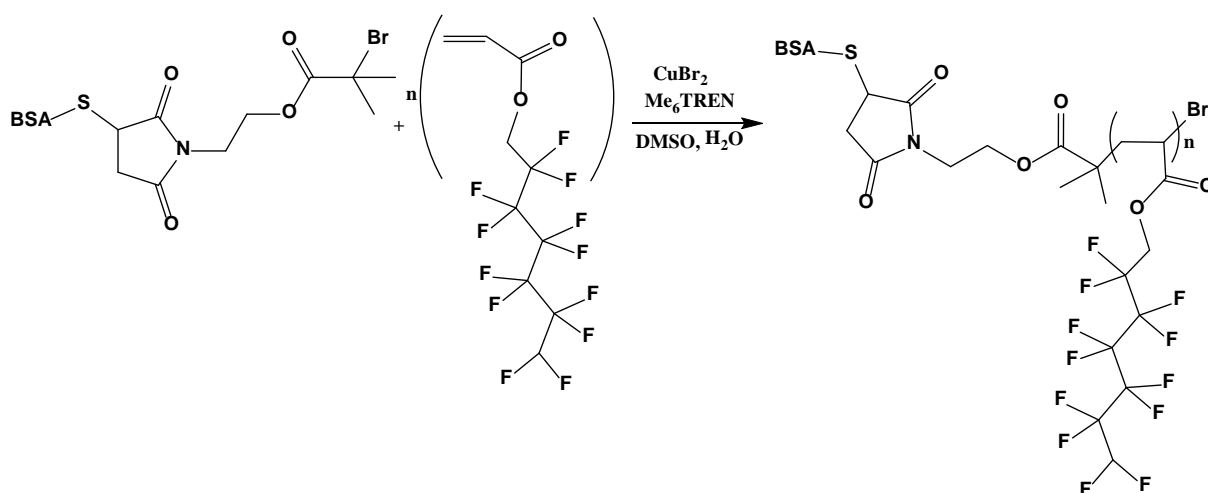


Figure 32. Electrophoretic behavior of BSA-poly(DFHA)

4.11 Photo-induced LRP grafting of 2,2,3,3,4,4,5,5,6,6,7,7-Dodecafluoroheptyl acrylate (DFHA) from BSA- macroinitiator **5** – Synthesis of BSA-poly(DFHA)



Scheme 14. Synthesis of BSA-poly(DFHA).

We conducted the same synthesis utilizing the photo-induced LRP grafting method as well. For this purpose a solution of BSA-macroinitiator **5** (1 equiv.) and a stirrer were placed in a milliliter syringe. Then the monomer 2,2,3,3,4,4,5,5,6,6,7,7-dodecafluoroheptyl acrylate (2000 equiv.) was dissolved in a mixture of 0.42 ml water and 0.2 ml DMSO. A solution of Me₆TREN (120 equiv) and CuBr₂ (15 equiv) in 1 ml of nanopure water was also prepared. Firstly, the monomer solution was added to the initiator solution and then 100 μl of the aqueous solution containing CuBr₂ and Me₆TREN were quickly added while the headspace

air was removed. A light blue color was immediately observed and great care was given in order to avoid air bubbles and eliminate the reaction headspace. The syringe was fitted with a rubber septum, placed under a UV nail lamp (365 nm), and the reaction mixture was left under stirring, for about 6 hours.

The crude polymerization mixture was extensively dialyzed initially against 5 mM phosphate buffer 7.4, 10% MeCN and EDTA overnight, another one dialysis against 5 mM phosphate buffer 7.4 for 2 hours and finally against 20 mM phosphate buffer 7.4 for 2 hours. After the purification, the product was studied with PAGE-electrophoresis (Figure 33). The appearance of new dark blue bands in the well of the stacking gel slightly migrating within the stacking gel combined with the negligibly dense the band of the biomacroinitiator **5** indicated that the reaction was almost quantitative.

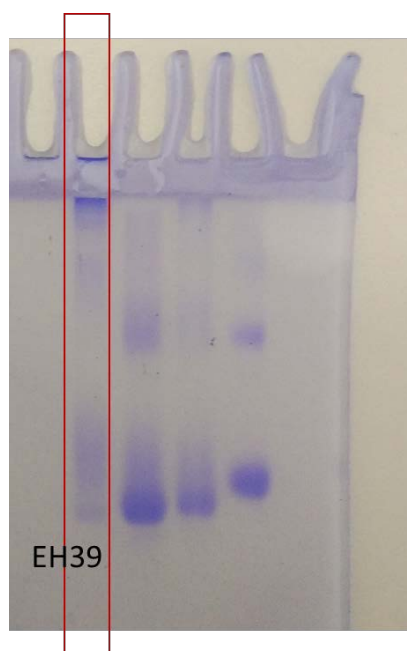


Figure 33. Electrophoretic behavior of BSA-poly(DFHA)

What is more, the formation of the bioconjugate was also indicated by GPC chromatography (Figure 34). The GPC chromatograms showed that in E39 experiment the polymerization was successful due to the faster elution of the bioconjugates when compared to the elution of the bioinitiator under the same conditions, indicating that it does have higher molecular weight.

Finally the product was analyzed with ^{19}F -NMR (Figure 35) where the characteristic peaks of CF_2 groups appear as singlets between -120 and -140 ppm. The final product contained six different CF_2 groups and therefore we observed six peaks in the NMR spectrum. FTIR spectroscopy (Figure 36) showed that there is a peak at 1276 cm^{-1} , representative for the successful formation of the corresponding polymers. In order to verify this indication we have

to synthesize the corresponding polymer without the BSA protein and compare the two FTIR spectra. From the above one can conclude that the photo-induced LRP grafting was proven to be more efficient in the case of this particular bioconjugate.

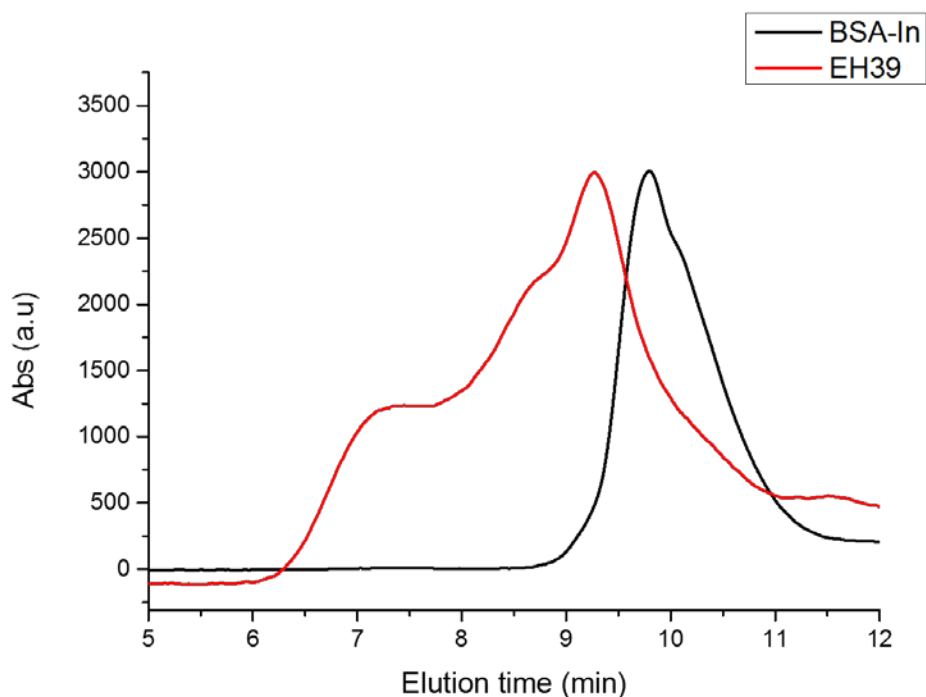


Figure 34. GPC Spectrum of BSA-macroinitiator 5 (BSA-In) and bioconjugate BSA-poly(DFHA).

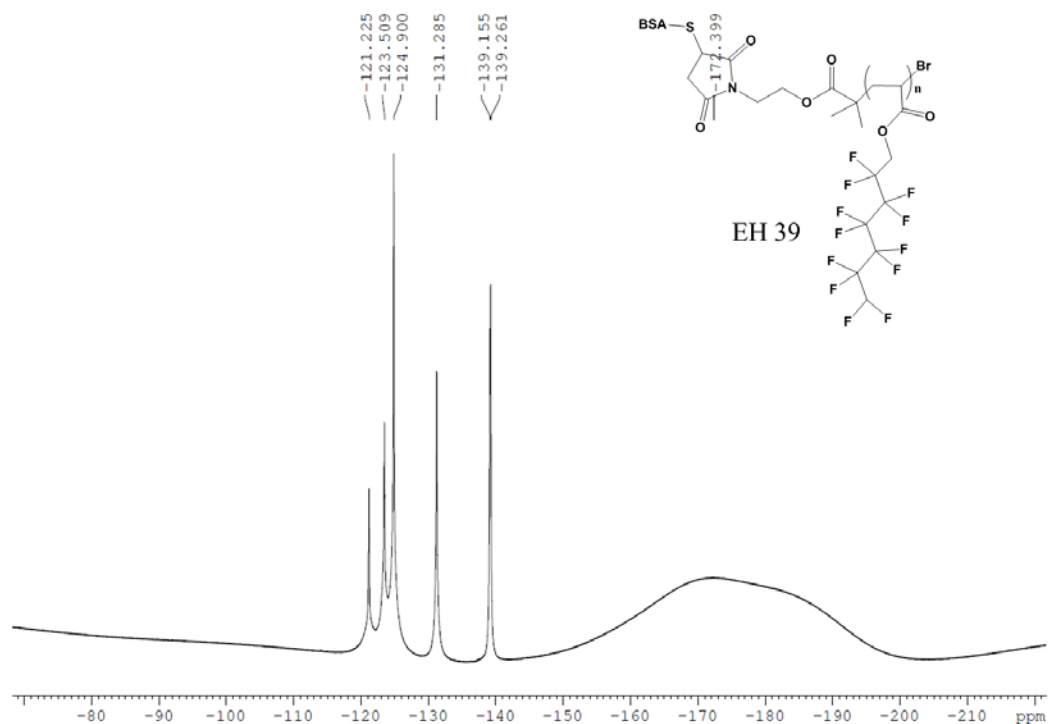


Figure 35. ^{19}F NMR Spectrum of BSA-poly(DFHA) polymer.

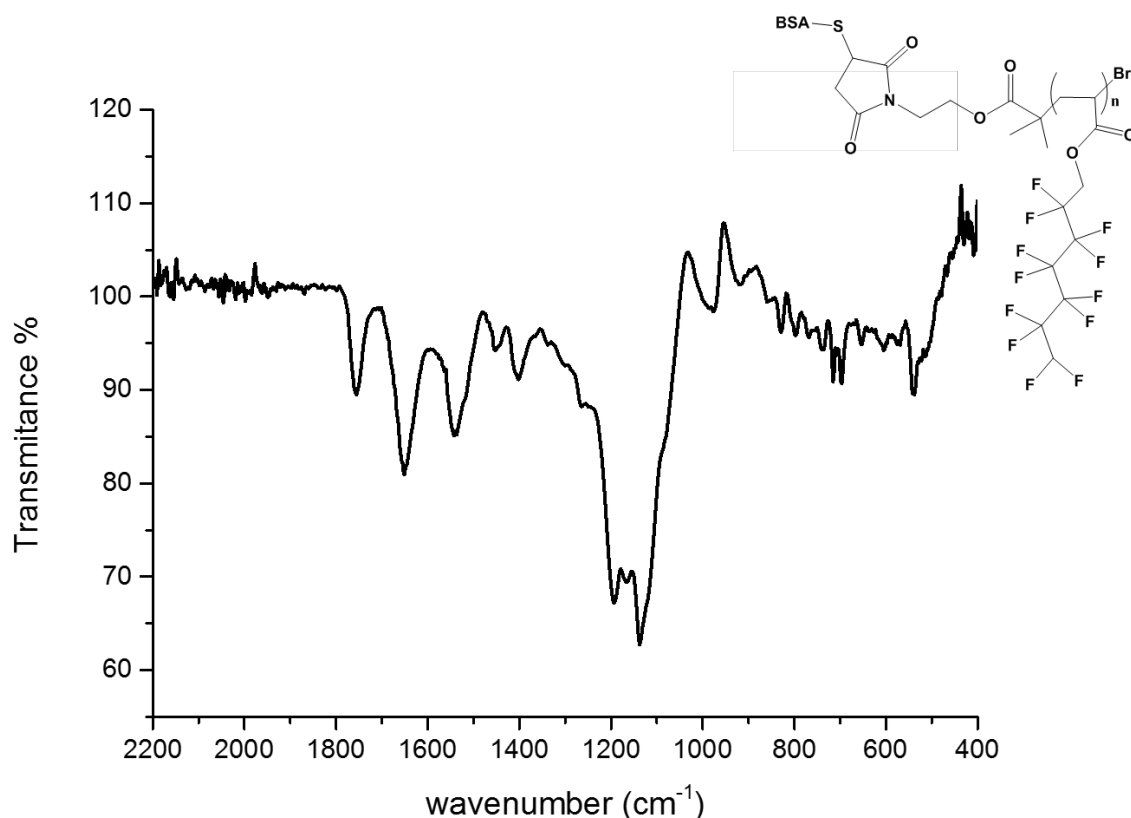
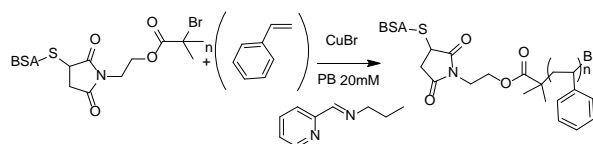


Figure 36. IR Spectrum of BSA-poly(DFHA) polymer.

4.12 Grafting of styrene from BSA-macroinitiator 5 – Synthesis of BSA-PS following ATRP without applying any deoxygenation



Scheme 15. Synthesis of BSA-polystyrene.

The last monomer that was studied during the current thesis is a common non-fluorinated monomer, styrene. Styrene was investigated with ATRP without the freeze pump thaw method in order to test whether it works and has acceptable yield. For the synthesis of BSA-polystyrene the amount of styrene ligand (2000 equiv.), N(Propyl)-2-pyridylmethanimine (70 equiv.) and CuBr (41 equiv.) were placed in an eppendorf and dissolved in 2 ml 20 mM phosphate buffer pH 7.4, 10% DMSO. The polymerization was triggered by transferring the monomer solution in a plastic syringe containing the crystalline BSA-macroinitiator **5** (1 equiv.). A light brown colour was immediately observed. The reaction mixture was stirred overnight at room temperature. The headspace of the syringe was eliminated. The crude polymerization mixture was purified by dialysis: initially against 5 mM phosphate buffer 7.4,

EDTA and 10% MeCN overnight, another one dialysis against 5 mM phosphate buffer 7.4 for 2 hours and finally against 20 mM phosphate buffer 7.4 for 2 hours. After the purification, the product was examined with PAGE-electrophoresis and GPC (Figures 37 and 38).

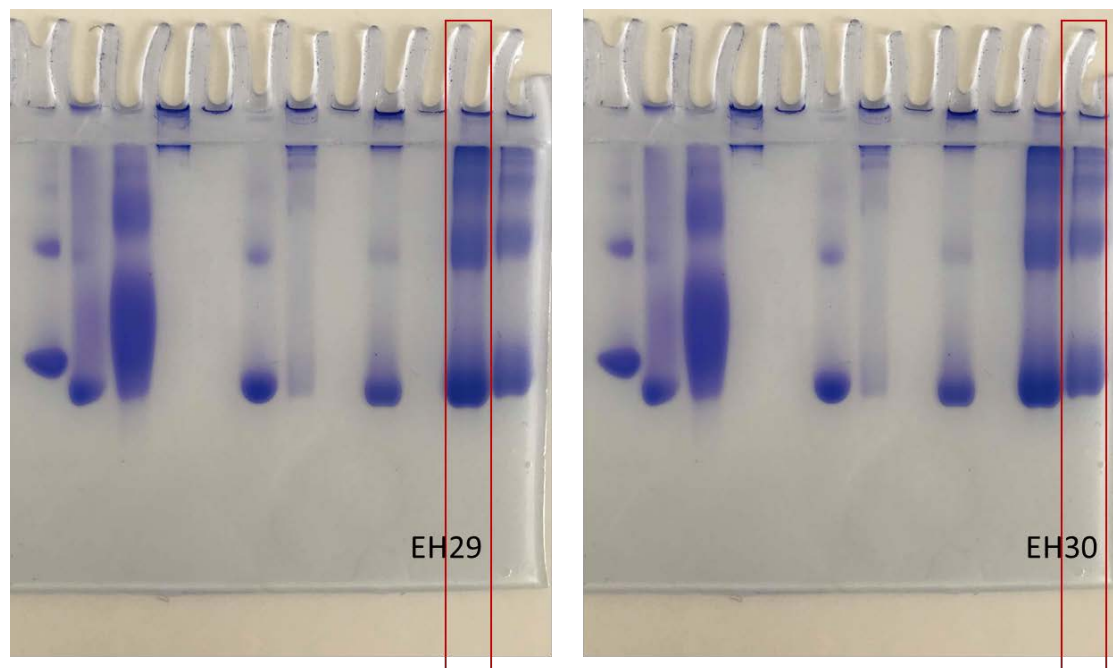


Figure 37. Electrophoretic behavior of BSA-polystyrene synthesized in two independent reactions.

In the PAGE-electrophoresis, the appearance of new dark blue bands in the well of the stacking gel slightly migrating within the stacking gel show the formation of the polymer product but the dense band of the biomacroinitiator **5** indicates that the reaction was not quantitative.

The GPC chromatograms showed that the EH27 experiment lead to some polymerization since there is a shoulder band appearing at shorter elution time. However the presence of significant amount of biomacroinitiator **5** is also observed, proving that the reaction was not succesful.

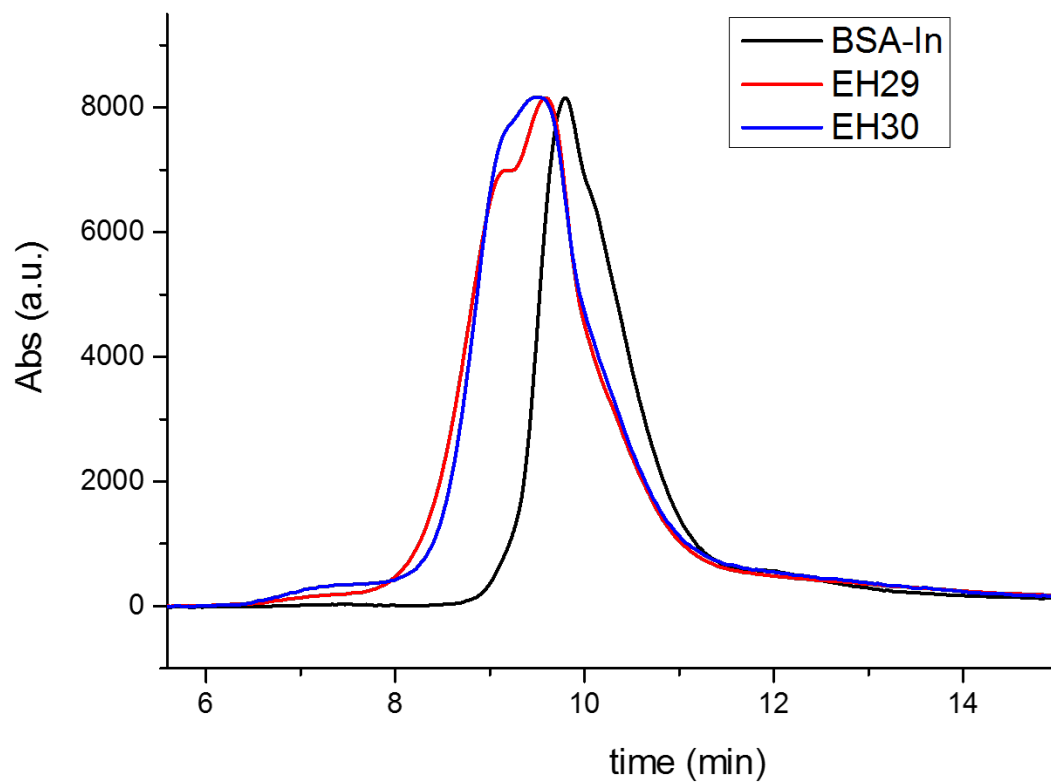


Figure 38. GPC Spectrum of BSA-macroinitiator 5 (BSA-In) and bioconjugate BSA-polystyrene from two independent reactions.

Chapter 5: Conclusions

The aim of this Bachelor thesis was to create giant amphiphilic bioconjugates consisting of a protein and a fluorinated polymer following oxygen tolerant polymerization protocols. To achieve our goals we applied two different synthetic approaches, namely SET-LRP and Photo-induced-LRP grafting of fluorinated monomers *from*²⁸ a protein-initiator. BSA along with a variety of fluorinated (with different number of fluorine atoms) and non-fluorinated monomers were used as building blocks for our synthetic approaches.

More specifically, three different fluorinated monomers were investigated for the formation of novel bioconjugates during the current thesis: 2,2,2-trifluoroethyl methacrylate, 2,2,2-trifluoroethyl acrylate, and 2,2,3,3,4,4,5,5,6,6,7,7-dodecafluoroheptyl acrylate. Additionally another non-fluorinated monomer was investigated utilizing an altered experimental procedure. More specifically we investigated whether ATRP could work using the syringe-system using styrene as a monomer. Previous experimental studies were verified through our experimental approach.²⁹ The synthesized protein polymer conjugates were fully characterized using various techniques such as PAGE electrophoresis, Gel Permeation Chromatography (GPC), Infrared Spectroscopy (IR), Scanning Electron Microscopy (SEM), ¹H-NMR and ¹⁹F-NMR Spectroscopy.

Our initial experiments aimed to the synthesis of the precursors necessary for the preparation of the BSA-macroinitiator **5**. The classical SET-LRP and photo-induced-LRP procedures were altered through the use of syringe in order to achieve elimination of the headspace of the reaction so only the dissolved oxygen remains in the reaction mixture. Rigorous deoxygenation methods were avoided through this novel approach. Therefore, we established a successful new synthetic approach which a more facile and quick method than the classical ATRP process. By comparing the two new synthetic protocols, one can conclude that photo-induced-LRP is more efficient, particularly in the cases of *BSA-poly(DFHA)* and *BSA-poly(TFEMA)*, than the SET-LRP method. More specifically the photo-induced-LRP procedure was successful for the synthesis of all protein polymer conjugates while the SET-LRP method succeeded only in the case of *BSA-poly(TFEA)*. When 2,2,2-trifluoroethyl methacrylate was used with the SET-LRP method, significant amount of bio-initiator was left unreacted and when 2,2,3,3,4,4,5,5,6,6,7,7-dodecafluoroheptyl acrylate was used with the same method there was no product at all.

Even though more studies have to be conducted for the further self-assembly characterization of these protein polymer conjugates, our investigation has opened new avenues to the synthesis fluorinated of fluorinated protein polymer conjugates.

Chapter 6: Experimental Part

6.1. Materials

All the reagents and materials used herein were purchased from the chemical companies Sigma- Aldrich, Fluka, Chemica, Acros Chemicals, Fischer Scientific and Alfa Aezar and were used without further purification. The Cellulose Dialysis Membranes for the purification of the bioconjugates were purchased by Spectrum Labs and had a MWCO of 10 kDa or 25kDa.

6.2. Analytical Methods

6.2.1. Nuclear magnetic resonance (NMR)

Nuclear Magnetic Resonance Spectroscopy is an excellent technique for determining the identity of a compound and proving the purity of the sample. In addition, it can be used to quantitative analyze mixtures containing known compounds. The high sensitivity and effectiveness of this technique makes it an essential tool for all synthetic chemists. The identity and purity of the compounds synthesized in this work were proved by ^1H - ^{13}C and ^{19}F - NMR spectroscopy measured on a Bruker AVANCE III-500 MHz spectrometer. The multiplicity of the peaks is described using the following abbreviations: s: singlet, d: doublet, t: triplet, m: multiplet.



6.2.2. Polyacrylamide gel Electrophoresis

Page Electrophoresis under standard non-denaturing conditions, was held in 4% stacking gel and 10% resolving gel, while the system that used were the Mini- PROTEANT Tetra Cell of BIO-RAD. The samples were dissolved in Premixed Sample Buffer for Native Page of BIO-RAD and were visualized with Coomassie Brilliant Blue.



6.2.3. Gel Permeation Chromatography (GPC)

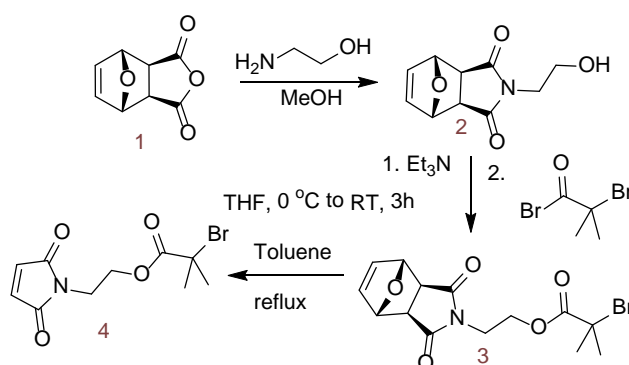
Gel permeation chromatography was used in order to characterize the bioconjugates using the Shimadzu VP HPLC system, which consist of a DGU-14A solvent degasser, an LC-10AD pump, a CTO-10A column oven, a SIL-10AD auto-injector, a RID-10A refractive index detector and a SPD-10A Shimadzu UV- Vis spectrometer. In the course of chromatography a 0.005 M phosphate buffer (pH 7.4) with 10% MeCN was used as the mobile phase A 0.35 mM BSA in 20mM phosphate buffer solution was used as a standard to whom all the other samples were compared.

6.2.4. Scanning Electron microscopy (SEM)

A scanning electron microscope (SEM) is a type of electron microscope that produces images of a sample by scanning the surface with a focused beam of electrons. The electrons interact with atoms in the sample, producing various signals that contain information about the sample's surface topography and composition. SEM experiments were performed at the Department of Biology of the University of Crete by using a JEOL JSM-6390LV microscope operating at 15 and 20kV.



6.3. Synthetic procedures



Scheme 16. Synthesis of the maleimido-initiator 4.

Maleimido-initiator 4 was synthesized twice during the current thesis as reported to literature.¹⁵

6.3.1 Synthesis of 4-(2-Hydroxyethyl)-10-oxa-4-aza-tricyclo[5.2.1.0^{2,6}]dec-8-ene-3,5-dione (2):

Initially the anhydride 1 (3a,4,7,7a-tetrahydro-4,7-epoxyisobenzofuran-1,3-dione, 2.00 g, 12.0 mmol) was suspended in MeOH (50 mL) and the mixture cooled to 0 °C. A solution of ethanolamine (0.71 mL, 12.0 mmol) in 20 mL of MeOH was added dropwise (over 10 min) in the reaction mixture which was stirred for 5 minutes at 0 °C. The mixture stirred at room temperature for 30 minutes, and then reflux conditions were applied for 4 h. After cooling the mixture to ambient temperature, the solvent was evaporated under reduced pressure and the white residue was dissolved in 50 mL of CH₂Cl₂ and washed 3 times with 20 ml of Brine solution. The organic layer was dried over MgSO₄, filtered and solvent was removed under reduced pressure providing a white-yellow residue. (0.767 gr, 3.67 mmol, 30.6% yield).

¹H NMR (500 MHz, CDCl₃, 298 K): δ = ~1.90 (bs, 1H, OH), 2.89 (s, 2H, CH), 3.69-3.71 (m, 2H, NCH₂), 3.75-3.78 (m, 2H, OCH₂), 5.28 (t, 2H, CH), 6.52 (t, 2H, CHvinyl).

6.3.2 Synthesis of 2-Bromo-2-methyl-propionic acid 2-(3,5-dioxo-10-oxa-4-aza-tricyclo[5.2.1.0^{2,6}]dec-8-en-4-yl)-ethyl ester (3)

The alcohol 2 (0.767 gr, 3.67 mmol) was dissolved in 40 ml THF and 0.56 ml of Et₃N (4 mmol) were added. The slightly turbid mixture was cooled to 0 °C and a solution of 2-bromo-isobutyryl-bromide (0.48 ml, 3.85 mmol) in 12.5 ml THF was added dropwise over 30 minutes. Afterwards the white suspension was stirred for 3 h at 0 °C and left overnight at

room temperature. TLC (P.E.:AcOEt) revealed the formation of the desired product. The ammonium salt byproduct was filtered off and the solvent removed under reduced pressure to give a pale-yellow residue.

In order to obtain the clean maleimido-protected initiator 3, a column chromatography with SiO₂ gel and petroleum ether/ethyl-acetate at 1:1 ratio solvent eluent was conducted to give the pale-yellow product 3.

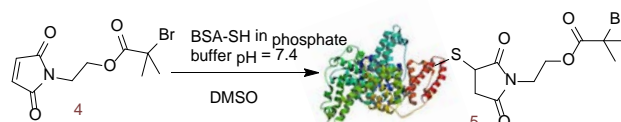
¹H NMR (500 MHz, CDCl₃, 298 K): δ = 1.89 (bs, 6H, CH₃), 2.86 (s, 2H, CH), 3.81 (t, 2H, NCH₂), 4.32 (t, 2H, OCH₂), 5.26 (m, 2H, CHO), 6.51 (m, 2H, CHvinyl).

6.3.3 Synthesis of 2-Bromo-2-methyl-propionic acid 2-(2,5-dioxo-2,5-dihydro-pyrrol-1-yl)-ethyl ester (4)

A solution of the maleimido-protected initiator 3 was suspended in toluene and reflux conditions were applied under nitrogen atmosphere overnight. Finally, the solvent was removed under reduced pressure to give the maleimido- initiator 4.

¹H NMR (500 MHz, CDCl₃, 298 K): δ = 1.86-1.95 (bs, 6H, CH₃), 3.84-3.87 (t, 2H, NCH₂), 4.32-4.34 (t, 2H, OCH₂), 6.74 (d, 2H, CHvinyl).

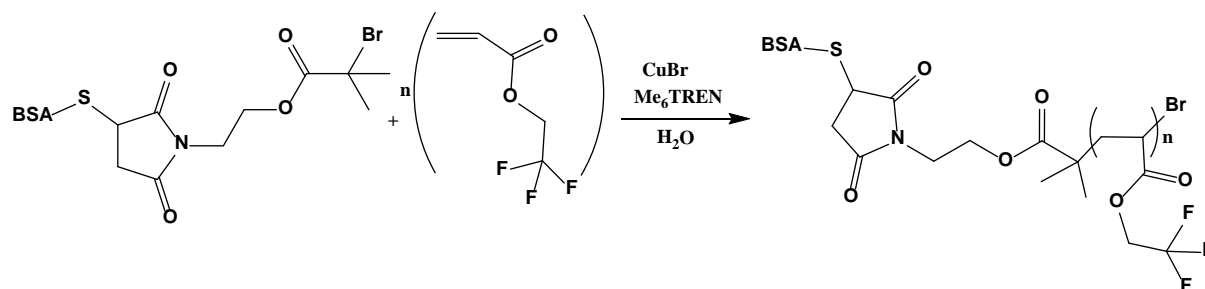
6.3.4 Synthesis of the BSA-macroiniator (5)



Scheme 17. Synthesis of BSA- macroiniator 5.

A solution of the maleimido-initiator 4 in DMSO (70 mM, 1 mL, 20 eq.) was prepared and slowly added in a 10 ml solution of BSA (0.35 mM, 1 eq.) in 20 mM phosphate buffer (pH 7.4). The reaction mixture was gently shaken for about 48 hours at ambient temperature. In order to eliminate the excess of the initiator 4, the mixture was extensively dialyzed initially against 5 mM phosphate buffer 7.4 ,10% MeCN and EDTA overnight, another one dialysis against 5 mM phosphate buffer 7.4 for 2 hours and finally against 20 mM phosphate buffer 7.4 for 2 hours (using regenerated cellulose dialysis membranes with a MWCO of 25 kDa). After that, the solution of the BSA macroiniator 5, was freeze dried and stored at -20 °C.

6.3.5 SET-LRP grafting of 2,2,2-trifluoroethyl acrylate (TFEA) from BSA-macroinitiator 5 – Synthesis of BSA-poly(TFEA)



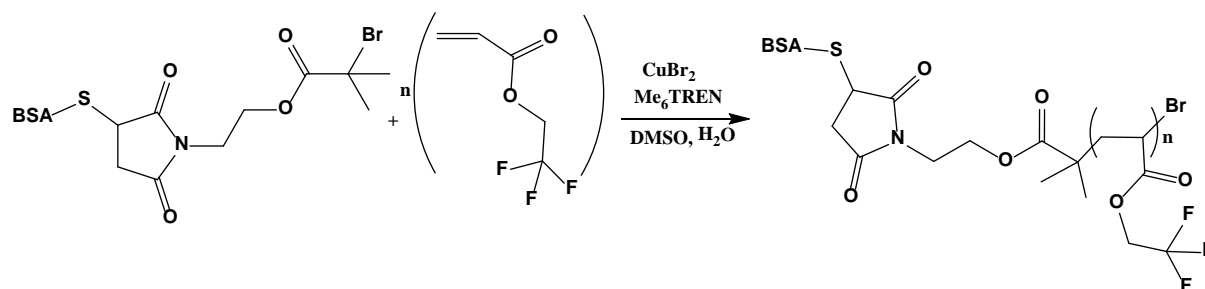
Scheme 18. Synthesis of BSA-poly(TFEA).

Initially CuBr (0.8 mg, 0.0059 mmol, 40 equiv.) and Tris[2-(dimethylamino)ethyl]amine (Me₆TREN) (0.00157 mL, 0.059 mmol, 40 equiv.) were dissolved in 0.37 mL H₂O and placed in a plastic syringe. The mixture was let under gentle stirring at 0 °C for 3 minutes for the activation of the copper catalyst. Subsequently BSA-macroinitiator **5** (0.42 ml, 0.00015 mmol, 1 equiv.) and 2,2,2-trifluoroethyl acrylate monomer (0.037 mL, 0.294 mmol, 2000 equiv.) were introduced to the mixture in the syringe and the reaction was stirred overnight at room temperature. The headspace of the syringe was eliminated in order to ensure the deoxygenated conditions that are required.

The crude polymerization mixture was purified by 3 dialysis. Initially a dialysis against 5 mM phosphate buffer 7.4, EDTA and 10% MeCN overnight, another one dialysis against 5 mM phosphate buffer 7.4 for 2 hours and finally against 20 mM phosphate buffer 7.4 for 2 hours were carried out. Regenerated cellulose dialysis membranes with MWCO 25 kDa were used for dialysis. After the purification, the product was characterized with PAGE-electrophoresis, GPC and ¹⁹F NMR.

¹⁹F NMR (500 MHz, D₂O, 298 K): δ = ~ -76 ppm

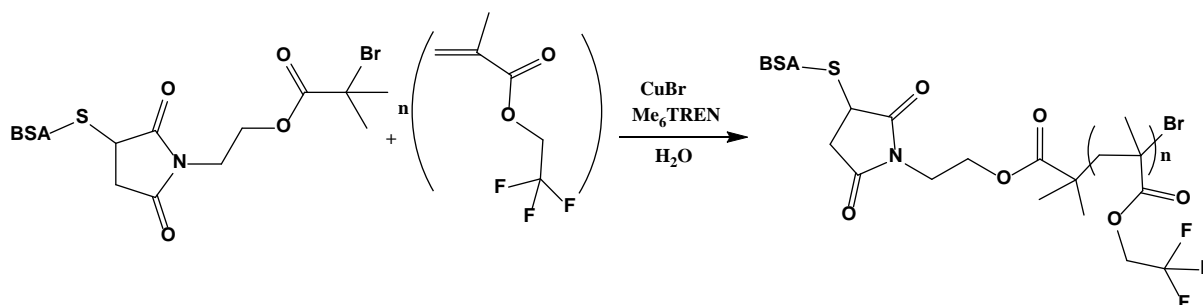
6.3.6 Photo-induced LRP grafting of 2,2,2-trifluoroethyl acrylate (TFEA) from BSA-macroinitiator 5 - BSA-poly(TFEA) – Synthesis of BSA-poly(TFEA)



Scheme 19. Synthesis of BSA-poly(TFEA).

A solution of BSA-macroinitiator **5** (1.25 ml, 0.000437 mmol, 1 equiv.) and a stirrer were placed in a milliliter syringe. Then the monomer 2,2,2-trifluoroethyl acrylate (TFEA) (0.11 ml, 0.874 mmol, 2000 equiv.) was dissolved in a mixture of 0.1 ml water and 0.2 ml DMSO. A solution of Me₆TREN (14 μl, 0.0524 mmol, 120 equiv) and CuBr₂ (1.5 mg, 0.00655 mmol, 15 equiv) in 1 ml of nanopure water was also prepared. Firstly, the monomer solution was added to the initiator solution using a Gilson pipette. Finally, 100 μl of the aqueous solution containing CuBr₂ and Me₆TREN were quickly added and air was removed. A light blue color was immediately observed and great care was given in order to avoid air bubbles and eliminate the reaction headspace. The syringe was fitted with a rubber septum, placed under a UV nail lamp (365 nm), and the reaction mixture was left under stirring, for about 8 hours. The crude polymerization mixture was extensively dialyzed initially against 5 mM phosphate buffer 7.4, 10% MeCN and EDTA overnight, another one dialysis against 5 mM phosphate buffer 7.4 for 2 hours and finally against 20 mM phosphate buffer 7.4 for 2 hours. After the purification, the product was studied with PAGE-electrophoresis.

6.3.7 SET-LRP grafting of 2,2,2-trifluoroethyl methacrylate from BSA-macroinitiator **5** – Synthesis of BSA-poly(TFEMA)



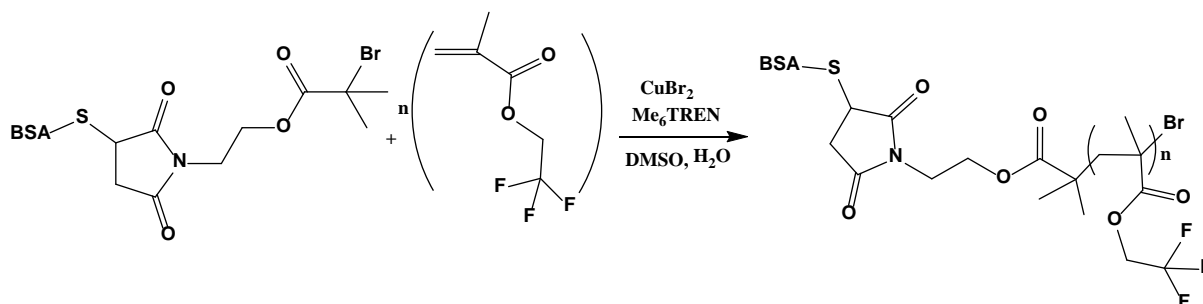
Scheme 20. Synthesis of BSA-poly(TFEMA).

Firstly the amounts of CuBr (0.8 mg, 0.0059 mmol, 40 equiv.) and Tris[2-(dimethylamino)ethyl]amine (Me₆TREN) (0.00157 mL, 0.059 mmol, 40 equiv.) were dissolved in 0.37 mL H₂O and placed in a plastic syringe. The mixture was stirred gently at 0 °C for 3 minutes for the activation of the copper catalyst. After that BSA-macroinitiator **5** (0.42 ml, 0.00015 mmol, 1 equiv.) and 2,2,2-trifluoroethyl methacrylate monomer (0.042 mL, 0.294 mmol, 2000 equiv.) were introduced to the mixture in the syringe and the reaction was left stirring overnight at room temperature. The use of the syringe provides oxygen-free conditions that are required. The crude polymerization mixture was purified by 3 dialysis: initially against 5 mM phosphate buffer 7.4, 10% MeCN and EDTA overnight, another one dialysis against 5 mM phosphate buffer 7.4 for 2 hours and finally against 20 mM phosphate

buffer 7.4 for 2 hours. Regenerated cellulose dialysis membranes with MWCO 25 kDa were used for dialysis. After the purification, the product was characterized with PAGE-electrophoresis, GPC and ^{19}F NMR.

^{19}F NMR (500 MHz, D_2O , 298 K): $\delta = -75$ ppm (s, 3F, CF_3).

6.3.8 Photo-induced LRP grafting of 2,2,2-trifluoroethyl methacrylate from BSA-macroinitiator **5** – Synthesis of BSA-poly(TFEMA)

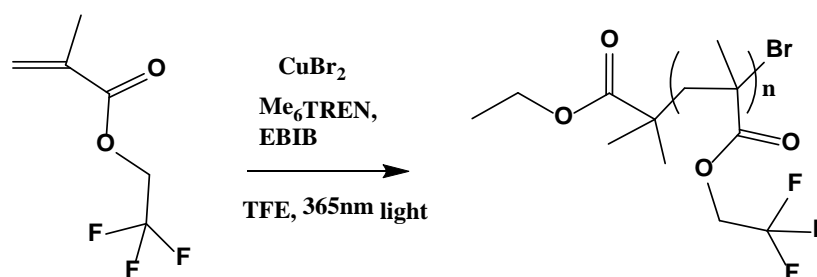


Scheme 21. Synthesis of BSA-poly(TFEMA).

A solution of BSA-macroinitiator **5** (1.25 ml, 0.000437 mmol, 1 equiv.) and a stirrer were placed in a milliliter syringe. Then the monomer 2,2,2-trifluoroethyl methacrylate (TFEMA) (0.12 ml, 0.874 mmol, 2000 equiv.) was dissolved in a mixture of 0.3 ml water and 0.2 ml DMSO. A solution of Me_6TREN (14 μl , 0.0524 mmol, 120 equiv) and CuBr_2 (1.5 mg, 0.00655 mmol, 15 equiv) in 1 ml of nanopure water was also prepared. Firstly, the monomer solution was added to the initiator solution using a glass pipette. Finally, 100 μl of the aqueous solution containing CuBr_2 and Me_6TREN were quickly added and air was removed. A light blue color was immediately observed and great care was given in order to eliminate the reaction headspace. The syringe was fitted with a rubber septum, placed under a UV nail lamp (365 nm) and the reaction mixture was left under stirring, for about 6 hours.

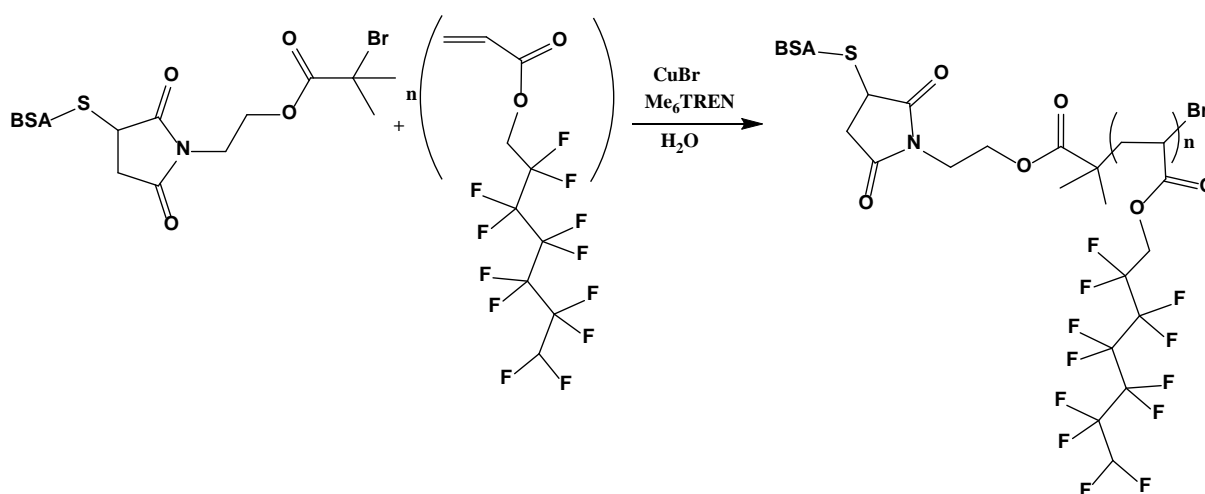
The crude polymerization mixture was extensively dialyzed initially against 5 mM phosphate buffer 7.4, EDTA and 10% MeCN overnight, another one dialysis against 5 mM phosphate buffer 7.4 for 2 hours and finally against 20 mM phosphate buffer 7.4 for another 2 hours. After the purification, the product was studied with PAGE-electrophoresis.

6.3.9 Photo-induced LRP grafting of 2,2,2-trifluoroethyl methacrylate from Ethyl α -bromoisobutyrate – Synthesis of poly(TFEMA)



The monomer 2,2,2-trifluoroethyl methacrylate (0.5 ml, 3.9 mmol, 50 equiv.) was added to a rubber septum-sealed vial equipped with a stirring magnet. A solution of Me_6TREN (2.5 μl , 0.009 mmol, 0.12 equiv) and CuBr_2 (0.35 mg, 0.002 mmol, 0.02 equiv) in 35 μl TFE was prepared and added to the vial followed by EBIB (11.5 μl , 0.08 mmol, 1 eq). The reaction mixture was purged with nitrogen for 10 min and placed under a UV lamp (365 nm) for 8h.

6.3.10 SET- LRP grafting of 2,2,3,3,4,4,5,5,6,6,7,7-Dodecafluoroheptyl acrylate (DFHA) from BSA- macroinitiator 5 – Synthesis of BSA-poly(DFHA)

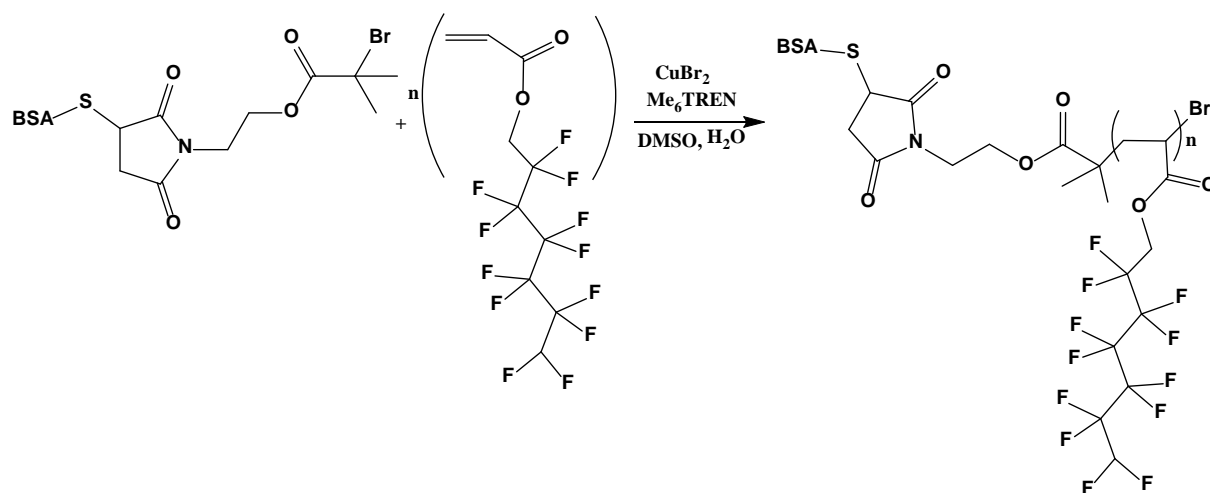


Scheme 22. Synthesis of BSA-poly(DFHA).

Initially CuBr (0.8 mg, 0.0059 mmol, 40 equiv.) and Tris[2-(dimethylamino)ethyl]amine (Me_6TREN) (0.00157 mL, 0.059 mmol, 40 equiv.) were dissolved in 0.37 mL deionized H_2O and placed in a plastic syringe. The mixture was let under gentle stirring at 0 $^\circ\text{C}$ for 3 minutes for the activation of the copper catalyst. Subsequently BSA-macroinitiator 5 (0.42 ml, 0.00015 mmol, 1 equiv.) and the monomer 2,2,3,3,4,4,5,5,6,6,7,7-dodecafluoroheptyl acrylate (0.072 mL, 0.294 mmol, 2000 equiv.) were introduced to the mixture in the syringe and the reaction was stirred overnight at room temperature. The use of the syringe ensures the deoxygenated conditions that are required.

The crude polymerization mixture was purified by 3 dialysis: initially against 5 mM phosphate buffer 7.4, 10% MeCN and EDTA overnight, another one dialysis against 5 mM phosphate buffer 7.4 for 2 hours and finally against 20 mM phosphate buffer 7.4 for 2 hours. Regenerated cellulose dialysis membranes with MWCO 25 kDa were used for dialysis. After the purification, the product was characterized with PAGE-electrophoresis, GPC and ^{19}F NMR.

6.3.11 Photo-induced LRP grafting of 2,2,3,3,4,4,5,5,6,6,7,7-dodecafluoroheptyl acrylate (DFHA) from BSA- macroinitiator – Synthesis of BSA-poly(DFHA)



Scheme 23. Synthesis of BSA-poly(DFHA).

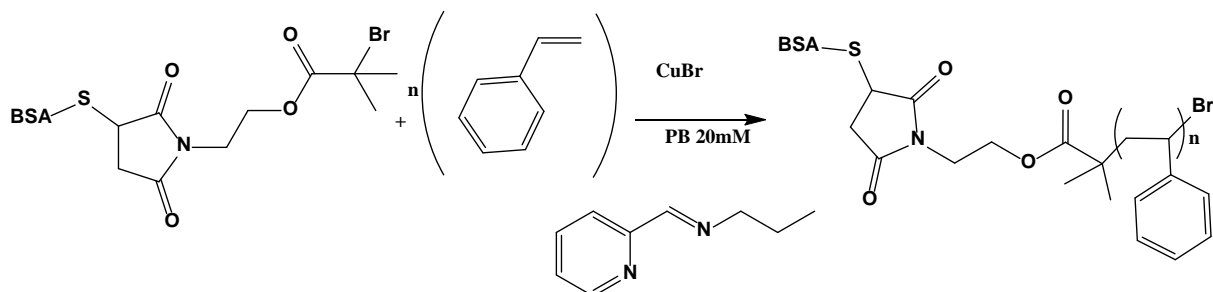
A solution of BSA-macroinitiator **5** (1.25 ml, 0.000437 mmol, 1 equiv.) and a stirrer were placed in a milliliter syringe. Then the monomer 2,2,3,3,4,4,5,5,6,6,7,7-Dodecafluoroheptyl acrylate (0.210 ml, 0.874 mmol, 2000 equiv.) was dissolved in a mixture of 0.42 ml water and 0.2 ml DMSO. A solution of Me_6TREN (14 μl , 0.0524 mmol, 120 equiv) and CuBr_2 (1.5 mg, 0.00655 mmol, 15 equiv) in 1 ml of nanopure water was also prepared. Firstly, the monomer solution was added to the initiator solution using a glass pipette.

Finally, 100 μl of the aqueous solution containing CuBr_2 and Me_6TREN were quickly added and air was removed. A light blue color was immediately observed and great care was given in order to avoid air bubbles and eliminate the reaction headspace. The syringe was fitted with a rubber septum, placed under a UV nail lamp (365 nm), and the reaction mixture was left under stirring, for about 6 hours.

The crude polymerization mixture was extensively dialyzed initially against 5 mM phosphate buffer 7.4, EDTA and 10% MeCN overnight, another one dialysis against 5 mM phosphate

buffer 7.4 for 2 hours and finally against 20 mM phosphate buffer 7.4 for another 2 hours. After the purification, the product was studied with PAGE-electrophoresis.

6.3.12 ATRP grafting of styrene from BSA-macroinitiator 5 – Synthesis of BSA-polystyrene



Scheme 24. Synthesis of BSA-polystyrene.

Styrene (0.080 ml, 0.7 mmol, 2000 equiv.), N(Propyl)-2-pyridylmethanimine (0.0036 ml, 0.0245 mmol, 70 equiv.) and CuBr (2 mg, 0.01435 mmol, 41 equiv) were placed in an eppendorf and dissolved in 2 ml 20 mM phosphate buffer pH 7.4, 10% DMSO. The polymerization was triggered by transferring the monomer solution in a plastic syringe tube containing the crystalline BSA-macroinitiator **5** (1 ml, 0.00035 mmol, 1 equiv.). The above procedure is changed compared to classical ATRP since a plastic syringe was used instead of a second schlenk tube. A light brown colour was immediately observed. The reaction mixture was stirred overnight at room temperature. The headspace of the syringe was eliminated. The crude polymerization mixture was purified by dialysis. Initially one dialysis against 5 mM phosphate buffer 7.4, EDTA and 10% MeCN overnight, another one dialysis against 5 mM phosphate buffer 7.4 for 2 hours and finally against 20 mM phosphate buffer 7.4 which left 2 hours. After the purification, the product was characterized with PAGE-electrophoresis and GPC.

Chapter 7: References

1. <https://www.scopus.com/>.
2. Xu, A.-H.; Zhang, L.-Q.; Ma, J.-C.; Ma, Y.-M.; Geng, B.; Zhang, S.-X., Preparation and surface properties of poly(2,2,2-trifluoroethyl methacrylate) coatings modified with methyl acrylate. *J. Coat. Technol. Res.* **2016**, *13*, 795-804.
3. Banerjee, S.; Tawade, B. V.; Améduri, B., Functional fluorinated polymer materials and preliminary self-healing behavior. *Polymer Chemistry* **2019**, *10*, 1993-1997.
4. Golichenari, B.; Velonia, K.; Nosrati, R.; Nezami, A.; Farokhi-Fard, A.; Abnous, K.; Behravan, J.; Tsatsakis, A. M., Label-free nano-biosensing on the road to tuberculosis detection. *Biosens. Bioelectron.* **2018**, *113*, 124-135.
5. Koda, Y.; Terashima, T.; Maynard, H. D.; Sawamoto, M., Protein storage with perfluorinated PEG compartments in a hydrofluorocarbon solvent. *Polymer Chemistry* **2016**, *7* (44), 6694-6698.
6. Wang, K.; Peng, H.; Thurecht, K. J.; Puttick, S.; Whittaker, A. K., Multifunctional hyperbranched polymers for CT/19F MRI bimodal molecular imaging. *Polymer Chemistry* **2016**, *7* (5), 1059-1069.
7. Cardoso, V. F.; Correia, D. M.; Ribeiro, C.; Fernandes, M. M.; Lanceros-Mendez, S., Fluorinated Polymers as Smart Materials for Advanced Biomedical Applications. *Polymers* **2018**, *10*, 1-26.
8. Darrell D. Ebbing, S. D. G., *General Chemistry*. Houghton Mifflin Company: 2009.
9. Peters, D., Problem of the Lengths and Strengths of Carbon—Fluorine Bonds. *J. Chem. Phys.* **1963**, *38*, 561-563.
10. Velonia, K.; Cornelissen, J. J. L. M.; Feiters, M. C.; Rowan, A. E.; Nolte, R. J. M., Aggregation of Amphiphiles as a Tool to Create Novel Functional Nano-Objects. *Nano. Sci. and Tech.* **2005**, 119-185.
11. Vriezema, D. M.; Hoogboom, J.; Velonia, K.; Takazawa, K.; Christianen, P. C.; Maan, J. C.; Rowan, A. E.; Nolte, R. J., Vesicles and polymerized vesicles from thiophene-containing rod-coil block copolymers. *Angew Chem Int Ed Engl* **2003**, *42*, 772-776.
12. Alexandridis P, L. B., Amphiphilic Block Copolymers: Self-assembly and applications. *Elsevier Science B V.* **2000**, *Amsterdam*.
13. Velonia, K.; Rowan, A. E.; Nolte, R. J., Lipase polystyrene giant amphiphiles. *J. Am. Chem. Soc.* **2002**, *124*, 4224-4225.

14. Koda, Y.; Terashima, T.; Sawamoto, M.; Maynard, H. D., Amphiphilic/fluorous random copolymers as a new class of non-cytotoxic polymeric materials for protein conjugation. *Polymer Chemistry* **2015**, *6*, 240-247.
15. Le Droumaguet, B.; Velonia, K., In situ ATRP-mediated hierarchical formation of giant amphiphile bionanoreactors. *Angew Chem Int Ed Engl* **2008**, *47*, 6263-6.
16. Le Droumaguet, B.; Velonia, K., Click Chemistry: A Powerful Tool to Create Polymer-Based Macromolecular Chimeras. *Macromol. Rapid Commun.* **2008**, *29* (12–13), 1073-1089.
17. Koda, Y.; Terashima, T.; Sawamoto, M., Multimode Self-Folding Polymers via Reversible and Thermoresponsive Self-Assembly of Amphiphilic/Fluorous Random Copolymers. *Macromolecules* **2016**, *49* (12), 4534-4543.
18. (a) Messina, M. S.; Messina, K. M. M.; Bhattacharya, A.; Montgomery, H. R.; Maynard, H. D., Preparation of biomolecule-polymer conjugates by grafting-from using ATRP, RAFT, or ROMP. *Prog. Polym. Sci.* **2020**, *100*, 101186; (b) Discekici, E. H.; Anastasaki, A.; Kaminker, R.; Willenbacher, J.; Truong, N. P.; Fleischmann, C.; Oschmann, B.; Lunn, D. J.; Read de Alaniz, J.; Davis, T. P.; Bates, C. M.; Hawker, C. J., Light-Mediated Atom Transfer Radical Polymerization of Semi-Fluorinated (Meth)acrylates: Facile Access to Functional Materials. *J. Am. Chem. Soc.* **2017**, *139* (16), 5939-5945.
19. Zhang, S., Building from the bottom up. *Mater. Today* **2003**, *6* (5), 20-27.
20. Yan, X.; Zhu, P.; Li, J., Self-assembly and application of diphenylalanine-based nanostructures. *Chem. Soc. Rev.* **2010**, *39* (6), 1877-90.
21. Matyjaszewski, K., Atom Transfer Radical Polymerization (ATRP): Current Status and Future Perspectives. *Macromolecules* **2012**, *45* (10), 4015-4039.
22. Wang, J.-S.; Matyjaszewski, K., Controlled/"living" radical polymerization. atom transfer radical polymerization in the presence of transition-metal complexes. *J. Am. Chem. Soc.* **1995**, *117* (20), 5614-5615.
23. Gao, Y.; Zhao, T.; Wang, W., Is it ATRP or SET-LRP? part I: Cu⁰&Cu^{II}/PMDTA – mediated reversible – deactivation radical polymerization. *RSC Adv.* **2014**, *4* (106), 61687-61690.
24. Percec, V.; Guliashvili, T.; Ladislaw, J. S.; Wistrand, A.; Stjerndahl, A.; Sienkowska, M. J.; Monteiro, M. J.; Sahoo, S., Ultrafast synthesis of ultrahigh molar mass polymers by metal-catalyzed living radical polymerization of acrylates, methacrylates, and vinyl chloride mediated by SET at 25 degrees C. *J. Am. Chem. Soc.* **2006**, *128* (43), 14156-65.

25. Lligadas, G.; Grama, S.; Percec, V., Single-Electron Transfer Living Radical Polymerization Platform to Practice, Develop, and Invent. *Biomacromolecules* **2017**, *18* (10), 2981-3008.
26. Frick, E.; Anastasaki, A.; Haddleton, D. M.; Barner-Kowollik, C., Enlightening the Mechanism of Copper Mediated PhotoRDRP via High-Resolution Mass Spectrometry. *J. Am. Chem. Soc.* **2015**, *137* (21), 6889-96.
27. Quan, Q.; Gong, H.; Chen, M., Preparation of semifluorinated poly(meth)acrylates by improved photo-controlled radical polymerization without the use of a fluorinated RAFT agent: facilitating surface fabrication with fluorinated materials. *Polymer Chemistry* **2018**, *9* (30), 4161-4171.
28. Velonia, K., Protein-polymer amphiphilic chimeras: recent advances and future challenges. *Polymer Chemistry* **2010**, *1* (7), 944.
29. (a) Spanos, L., Synthesis of protein-perfluorinated polymer bioconjugates. *Heraklion, Crete, University of Crete* **2018**; (b) Grafanaki, E. K., Synthesis of perfluorinated biopolymers. *Heraklion, Crete, University of Crete* **2018**.